

We are IntechOpen, the world's leading publisher of Open Access books Built by scientists, for scientists

6,900

Open access books available

186,000

International authors and editors

200M

Downloads

Our authors are among the

154

Countries delivered to

TOP 1%

most cited scientists

12.2%

Contributors from top 500 universities



WEB OF SCIENCE™

Selection of our books indexed in the Book Citation Index
in Web of Science™ Core Collection (BKCI)

Interested in publishing with us?
Contact book.department@intechopen.com

Numbers displayed above are based on latest data collected.
For more information visit www.intechopen.com



Visible Light-Driven Water Oxidation Catalyzed by Ruthenium Complexes

Markus D. Kärkäs, Tanja M. Laine,
Eric V. Johnston and Björn Åkermark

Additional information is available at the end of the chapter

<http://dx.doi.org/10.5772/62272>

Abstract

A shift in energy dependence from fossil fuels to sustainable and carbon-neutral alternatives is a daunting challenge that faces the human society. Light harvesting for the production of solar fuels has been extensively investigated as an attractive approach to clean and abundant energy. An essential component in solar energy conversion schemes is a catalyst for water oxidation. Ruthenium-based catalysts have received significant attention due to their ability to efficiently mediate the oxidation of water. In this context, the design of robust catalysts capable of driving water oxidation at low overpotential is a key challenge for realizing efficient visible light-driven water splitting. Herein, recent progress in the development within this field is presented with a focus on homogeneous ruthenium-based systems and surface-immobilized ruthenium assemblies for photo-induced oxidation of water.

Keywords: water splitting, ruthenium, photochemistry, sustainable chemistry

1. Introduction

The search for inexpensive and renewable energy is currently one of society's greatest technological challenges. As light energy from the sun continuously strikes the earth's surface, harnessing this energy would solve the increasing future energy demand and lead to a more sustainable society. An appealing solution would therefore be to convert light energy to storable fuels, such as hydrogen gas or reduced carbon compounds. For realizing this scenario, novel technologies have to be developed that efficiently utilize solar energy. Furthermore, such systems also need to rely on abundant and inexpensive feedstocks in order to become viable on a large

scale. As water is plentiful, it would be attractive to use it as a feedstock for obtaining the necessary reducing equivalents—protons and electrons [1–6].

The natural system constitutes an excellent source of inspiration for how to design an artificial system that is capable of harnessing solar energy for fuel production. The concept of artificial photosynthesis emerged in the 1970s and is inspired by nature where light-induced charge separation events sequentially oxidize a Mn_4Ca cluster (Figure 1) known as the oxygen-evolving complex (OEC) [7, 8]. After four electrons have been abstracted from the OEC, two molecules of water are oxidized to molecular oxygen, thus releasing four electrons and four protons. The natural photosynthetic apparatus subsequently utilizes the generated reducing equivalents to reduce CO_2 to carbohydrates [9, 10]. However, instead of using the generated reducing equivalents to reduce CO_2 to carbohydrates as in the natural photosynthetic apparatus, these “artificial leaves” would produce hydrogen gas from the protons and electrons that are liberated when water is oxidized (Eq. 1) [11, 12].

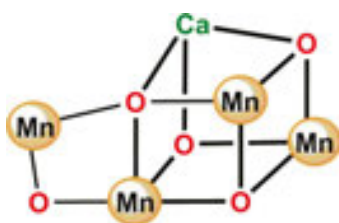


Figure 1. Depiction of the Mn_4Ca cubane core of the oxygen-evolving complex (OEC).

Water splitting can be divided into two half-reactions; proton reduction and water oxidation. The reductive side of water splitting involves the generation of hydrogen gas from the generated protons and electrons. In contrast to hydrocarbons, hydrogen gas is considered to be environmentally benign, as water is the only combustion product. Although deceptively simple, the other half-reaction, water oxidation (Eq. 2), is a mechanistically complex process and is currently considered as the bottleneck. The oxidation of water thus requires a single catalytic entity capable of accumulating four oxidizing equivalents, breaking several bonds and forming the crucial O–O bond. Splitting of water is an energy demanding process with a Gibbs free energy of $237.18 \text{ kJ mol}^{-1}$ and a minimum electrochemical potential of 1.229 V vs. normal hydrogen electrode (NHE) is required. The basic thermodynamic requirements for splitting water suggest that any light with a wavelength shorter than 1 μm has enough energy to split a molecule of water. Consequently, this allows the use of the entire visible solar spectrum and a majority of the near-infrared spectrum, which collectively constitutes ~80% of the total solar irradiance [13].



The first example of photoelectrochemical water splitting was reported by Fujishima and Honda in the early 1970s. Their system consisted of a titanium dioxide (TiO_2) photoanode which upon irradiation with ultraviolet (UV) light generated oxygen at the anode and hydrogen gas at an unilluminated platinum cathode [14]. Since the seminal work by Fujishima and Honda, several research groups have attempted to improve the system in order to enable the reaction to be driven by visible light instead of UV light [15, 16].

A simple depiction of an artificial photosynthetic system is shown in Figure 2 and consists of three components: a chromophore (photosensitizer) for light-absorption, a water oxidation catalyst (WOC), and a reduction catalyst for proton reduction. The light-absorbing component, the molecular chromophore, is in general coordinated to the surface of a semiconductor, such as TiO_2 . The initial step in such a system involves light absorption by the photosensitizer, generating a long-lived charge-separated state by transferring an electron to the conduction band of the semiconductor. The oxidized photosensitizer subsequently recovers an electron from the covalently bound oxidation catalyst (the WOC) or from the functionalized semiconductor surface to regenerate the ground state photosensitizer. After four successive electron transfers, the highly oxidized WOC is reduced by oxidizing two molecules of water, thus releasing molecular oxygen. Although the events seem trivial, the overall process of light-driven water splitting requires interfacing of several nontrivial chemical steps such as accumulation and abstraction of several electrons at the reduction and oxidation catalyst, respectively. This requires the integration of efficient light absorption, generation of long-lived charge separation, organized proton reduction at the cathode, and fast oxidation of water at the anode [17–19].

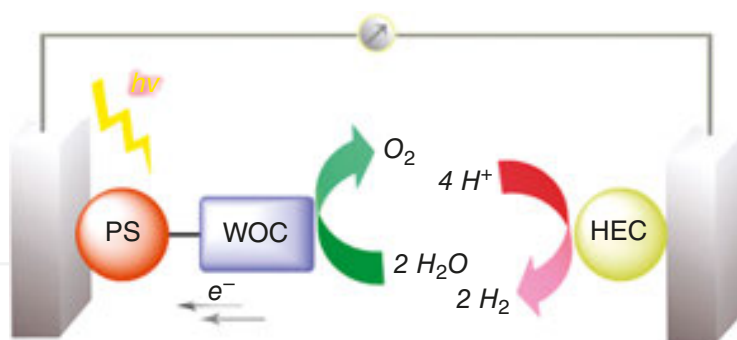


Figure 2. Three-component molecular assembly for water splitting consisting of a photosensitizer (PS), a water oxidation catalyst (WOC), and a hydrogen-evolving catalyst (HEC). Reprinted with permission from ref. 29. Copyright 2014 American Chemical Society.

2. Ruthenium-Based Photosensitizers

The first step in solar energy conversion schemes involves light absorption by a chromophore. In the natural photosynthetic system, a set of specialized chlorophyll-based pigments is responsible for the absorption of visible light, and subsequently transfers the excitation energy

to the reaction centers of photosystem II and I. Mimicking these events for constructing artificial photosynthetic devices is a crucial objective and requires tailored photosensitizers that are photostable and efficiently absorb photons across a wide range of wavelengths in the visible spectral region. Furthermore, they should also be easy to modify to allow for straightforward tuning of the photophysical features. The main requirement is that the reduction potential of the oxidized photosensitizer is more positive than that of the WOC and the onset potential for water oxidation (and any overpotential that is produced in the designed system) [20, 21].

2.1. Photophysical Description of Ruthenium-Type Photosensitizers

Perhaps the most extensively studied metal-based photosensitizers are the $[\text{Ru}(\text{bpy})_3]^{2+}$ -type complexes (Figure 3; bpy = 2,2'-bipyridine). Shortly after the seminal report on UV-light-mediated water splitting at TiO_2 photoanodes by Honda and Fujishima [14], the basis for artificial photosynthesis appeared when it was realized that metal complexes, such as $[\text{Ru}(\text{bpy})_3]^{2+}$ (1), are efficiently quenched by organic compounds [22, 23]. Flash photolysis experiments have revealed that light absorption ($\lambda_{\text{max}} \approx 450 \text{ nm}$) by the $[\text{Ru}(\text{bpy})_3]^{2+}$ -type photosensitizers triggers excitation of an electron in a metal-centered orbital to a π^* orbital located on the ancillary polypyridyl ligand. This metal-to-ligand charge transfer (MLCT) results in a singlet excited state, $^1[\text{Ru}(\text{bpy})_3]^{2+*}$, that undergoes rapid intersystem crossing (ISC), affording a triplet state, $^3[\text{Ru}(\text{bpy})_3]^{2+*}$. This excited state is relatively long lived and has a dual nature, being that it can participate in either a single-electron oxidation or a single-electron reduction in the presence of an acceptor or a donor, respectively (Figure 4). The $[\text{Ru}(\text{bpy})_3]^{2+}$ -type photosensitizers possess several desirable features: 1) photostability, 2) the produced excited state has a sufficient lifetime for it to participate in chemical reactions, 3) they exhibit compatibility with a wide pH range, 4) they display broad absorption of visible light, and 5) the relative ease by which the photophysical properties of the ruthenium photosensitizers can be tuned, allowing e.g. that the absorption of light can be extended from the near infrared to the UV region by simply modifying the ancillary ligands (see Figure 3) [24–26].

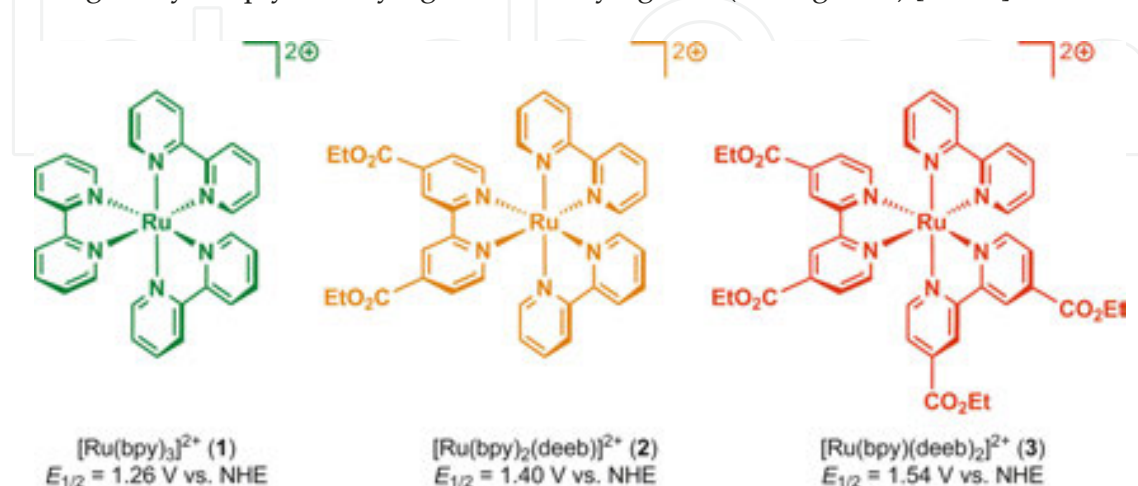


Figure 3. Examples of $[\text{Ru}(\text{bpy})_3]^{2+}$ -type photosensitizers.

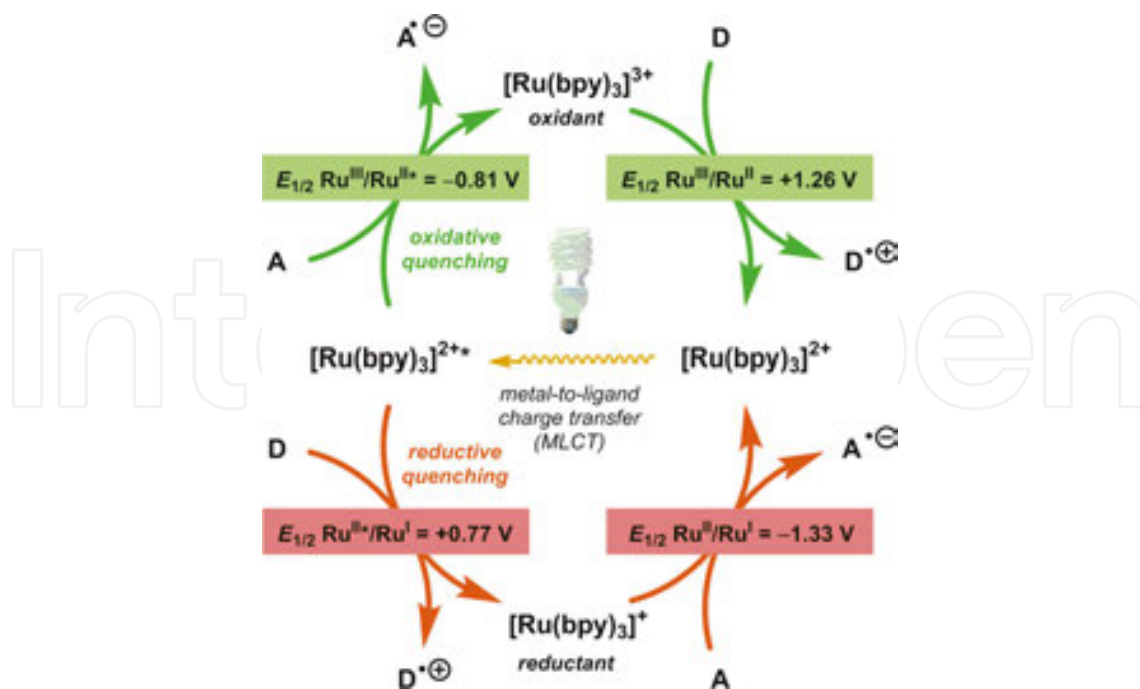


Figure 4. Photophysical properties of the $[\text{Ru}(\text{bpy})_3]^{2+}$ complex (1).

2.2. Evaluating Light-Driven Water Oxidation with Ruthenium Complexes

A three-component system is typically employed for evaluating light-driven water oxidation and consists of a photosensitizer, a water oxidation catalyst, and a sacrificial electron acceptor (Figure 5). As the sacrificial electron acceptor, sodium persulfate is usually employed since the recombination or reversed electron transfer can be ruled out, thereby simplifying the kinetic analysis of subsequent steps in the catalytic process. The three-component light-driven system using the persulfate anion ($\text{S}_2\text{O}_8^{2-}$) and a metal-based photosensitizer has been well documented and is believed to commence with oxidative quenching of the excited state of the photosensitizer, such as $[\text{Ru}(\text{bpy})_3]^{2+*}$. This results in the generation of $[\text{Ru}(\text{bpy})_3]^{3+}$, sulfate, and a sulfate radical ($\text{SO}_4^{\cdot-}$), which is a strong oxidant ($E^\circ > 2.40 \text{ V vs. NHE}$ [27]) and has the ability to directly oxidize a second equivalent of $[\text{Ru}(\text{bpy})_3]^{2+}$ [28]. The reduction of two equivalents affords the four equivalents of $[\text{Ru}(\text{bpy})_3]^{3+}$ that are needed to oxidize the WOC, which in turn oxidizes water to molecular oxygen. The processes involved in the light-driven persulfate system are summarized by Eqs. 3–6.

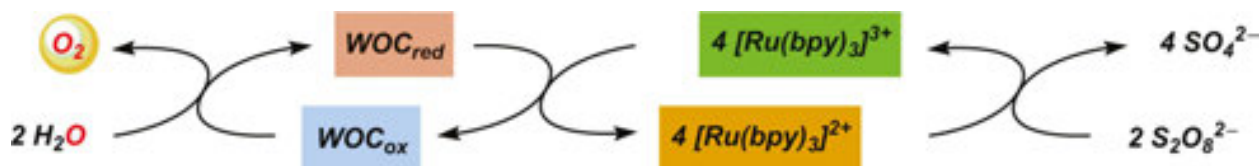
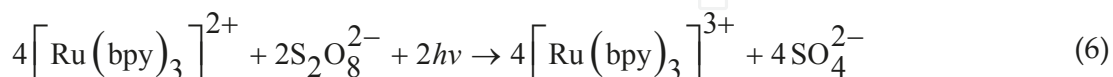
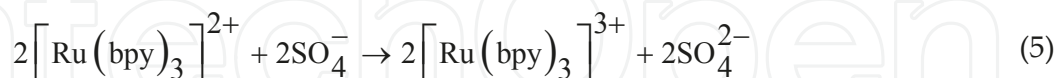
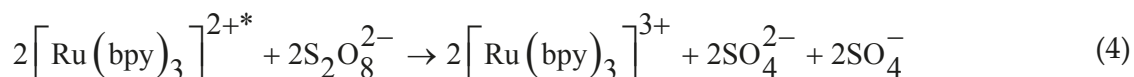
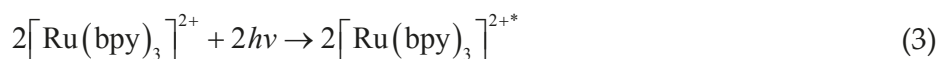


Figure 5. Three-component system for light-driven water oxidation consisting of a water oxidation catalyst, a $[\text{Ru}(\text{bpy})_3]^{2+}$ -type photosensitizer and persulfate as the sacrificial electron acceptor.



3. Ruthenium-Based Water Oxidation Catalysts—Oxidatively Robust Catalytic Entities

One of the main challenges in realizing water splitting is the development of efficient and robust WOCs that possess low overpotentials and high turnover rates. The development of homogeneous WOCs is an intense and rapidly expanding research field. During the past decade, considerable progress in constructing molecular catalysts capable of oxidizing water has been made using transition metal-based catalysts in the presence of strong chemical oxidants, such as Ce^{IV} [29, 30]. Homogeneous catalysts are advantageous as they facilitate mechanistic studies, thus stimulating the design of new and improved WOCs [31]. Owing to their high abundance and low toxicity, several WOCs based on first-row transition metals, such as cobalt (Figure 6) [32–35], copper (Figure 7) [36–38], iron (Figure 8) [39–42], and manganese (Figure 9) [43–47], have been designed. However, their design has proven particularly challenging as these WOCs suffer from insufficient stability and are rapidly deactivated/decomposed under the harsh conditions required to oxidize water. In contrast, catalysts based on the third-row transition metal ruthenium have shown to produce robust catalysts that are able to deliver high turnover numbers (TONs) and high turnover frequencies (TOFs) [29, 30]. This chapter summarizes the recent advances that have been made in designing ruthenium-based WOCs for visible light-driven water oxidation.

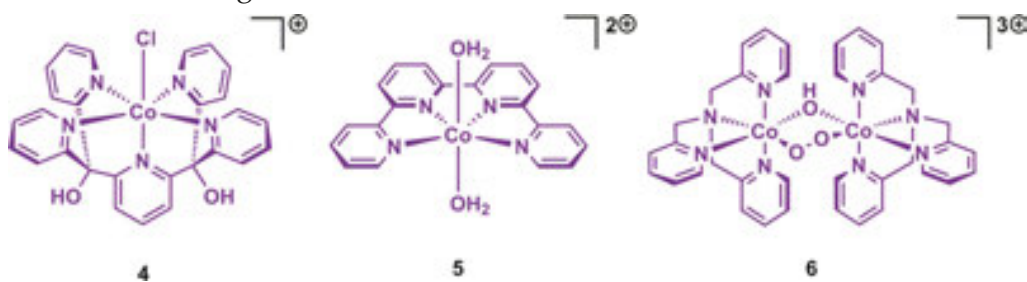


Figure 6. Examples of cobalt-based water oxidation catalysts.

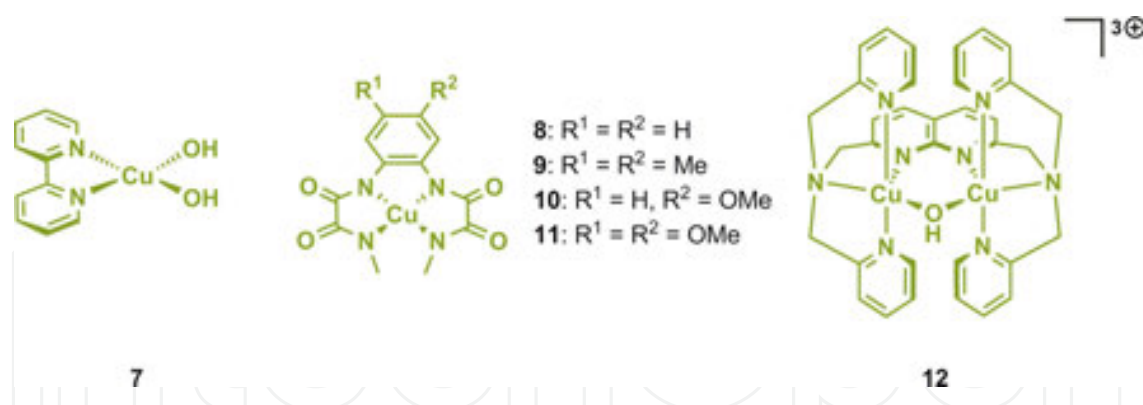


Figure 7. Examples of copper-based water oxidation catalysts.

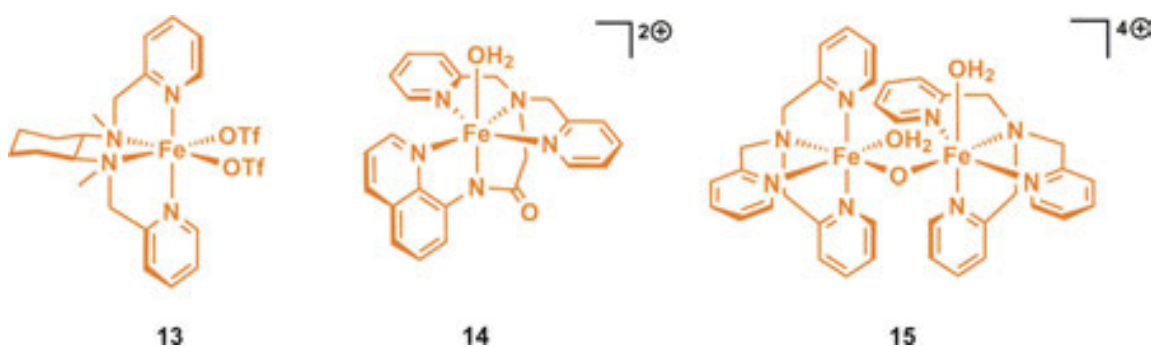


Figure 8. Examples of iron-based water oxidation catalysts.

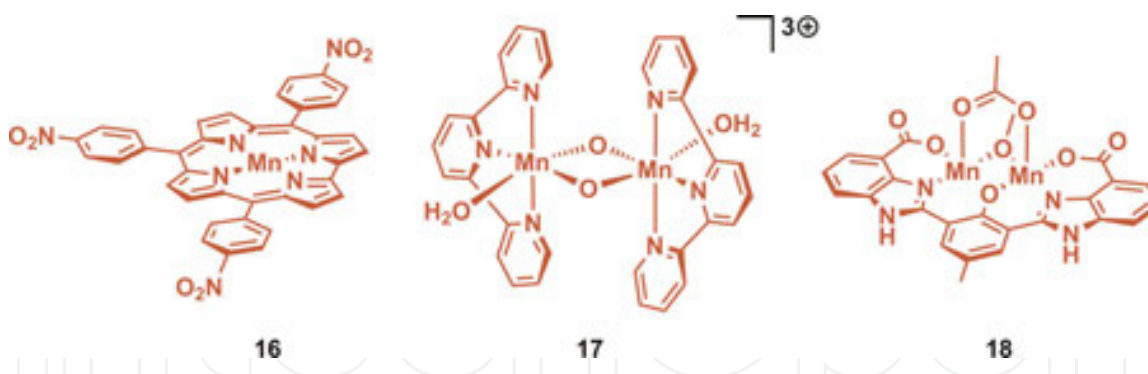


Figure 9. Examples of manganese-based water oxidation catalysts.

3.1. Dinuclear Ruthenium Complexes Capable of Mediating Light-Driven Water Oxidation

Intensive attempts to develop efficient WOCs have been made since the first homogeneous ruthenium catalyst, the “blue dimer” (19, Figure 10), was presented by Meyer and coworkers in the early 1980s [48, 49]. Light-driven water oxidation by a mononuclear “blue dimer”, *cis*-[(bpy)₂Ru(OH₂)₂]²⁺, derivative which presumably resulted in the formation of the dinuclear derivative 20 (Figure 10), was reported in 1987 [50]. In addition to the coordinated aqua ligands,

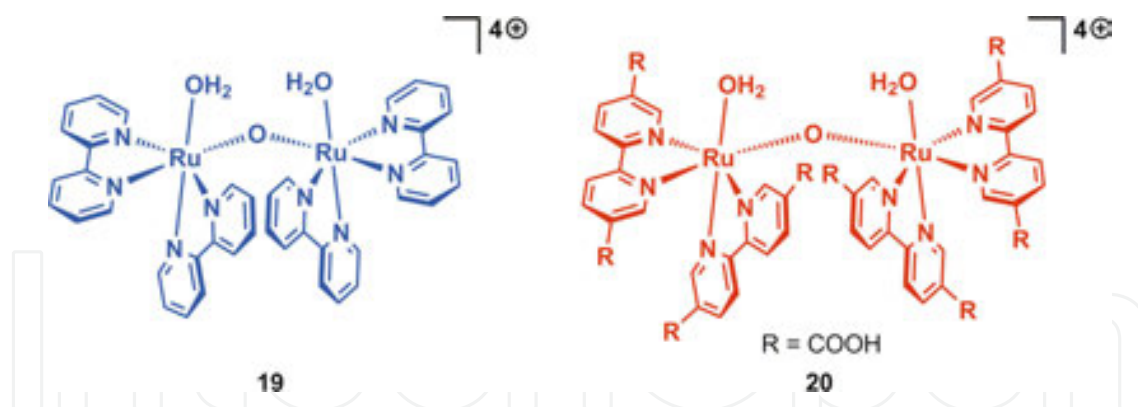


Figure 10. Depiction of the “blue dimer” (19) and dinuclear ruthenium complex 20.

this ruthenium-aqua complex consisted of two ruthenium metal centers connected via a μ -oxo bridge and two carboxylate substituted bpy ligands. Cyclic voltammetry displayed a reversible wave at ~ 1.20 V vs. NHE, assigned to the $\text{Ru}_2^{\text{III,IV}}/\text{Ru}_2^{\text{III,III}}$ redox couple and a catalytic onset for water oxidation at approximately 1.54 V vs. NHE. When using $[\text{Ru}(\text{deeb})_3]^{2+}$ as the photosensitizer and sodium persulfate as the sacrificial electron acceptor, molecular oxygen was evolved at a rate of $330 \mu\text{L h}^{-1}$ during the first 15 min, after which the oxygen production dropped.

The groups of Sun and Åkermark designed a dinuclear ruthenium complex (21, Figure 11) where the two ruthenium centers were positioned in an *anti*-fashion about a central pyridazine moiety [51]. In addition to the central pyridazine unit, the ligand scaffold contained two pyridine groups with negatively charged carboxylate groups, which have been shown to lower the redox potentials of metal complexes and stabilize high-valent redox states. The electrochemical properties of the complex were studied by cyclic voltammetry in dry acetonitrile and showed two reversible one-electron waves at ~ 0.54 and ~ 1.04 V vs. NHE, which were assigned as the $\text{Ru}_2^{\text{II,III}}/\text{Ru}_2^{\text{II,II}}$ and $\text{Ru}_2^{\text{III,III}}/\text{Ru}_2^{\text{II,III}}$ redox couples. At pH 7, a catalytic current for water oxidation was observed at ~ 1.45 V vs. NHE.

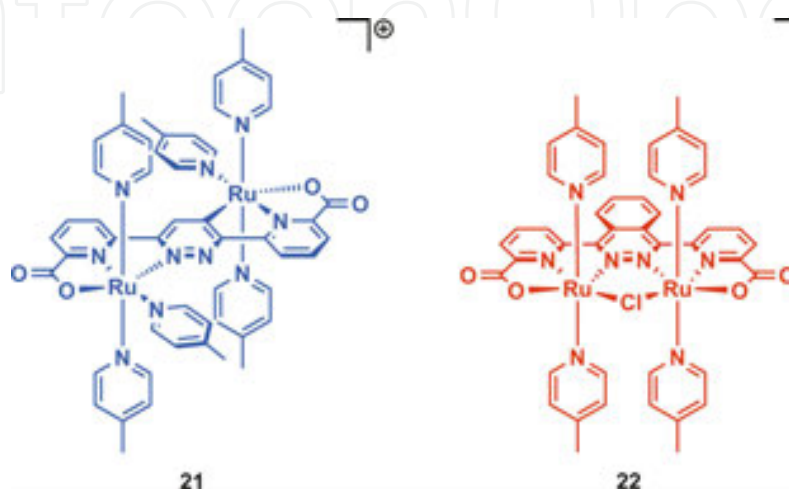


Figure 11. Structures of the dinuclear ruthenium complexes **21** and **22**.

Three different $[\text{Ru}(\text{bpy})_3]^{2+}$ -type photosensitizer derivatives were employed for visible light-driven water oxidation [52]. It could be shown that the TONs and TOFs increased with the increasing potential of the photosensitizer, which is ascribed to the stronger driving force. When employing the $[\text{Ru}(\text{bpy})(\text{deeb})_2]^{2+}$ photosensitizer, a TON of 370 and a TOF of 0.26 s^{-1} was obtained for ruthenium complex **21**. During the catalytic process, the pH was found to drop significantly and had to be adjusted. However, this allowed for a total TON of 1270 after four consecutive runs. Unfortunately, using a more concentrated buffer solution (0.2 M) resulted in deactivation of the catalytic system. In the presence of catalyst **21**, minimal decomposition of the photosensitizers was observed upon illumination, whereas in the absence of catalyst **21**, significant decomposition of the photosensitizers was observed, indicating efficient electron transfer from the catalyst unit to the oxidized photosensitizer.

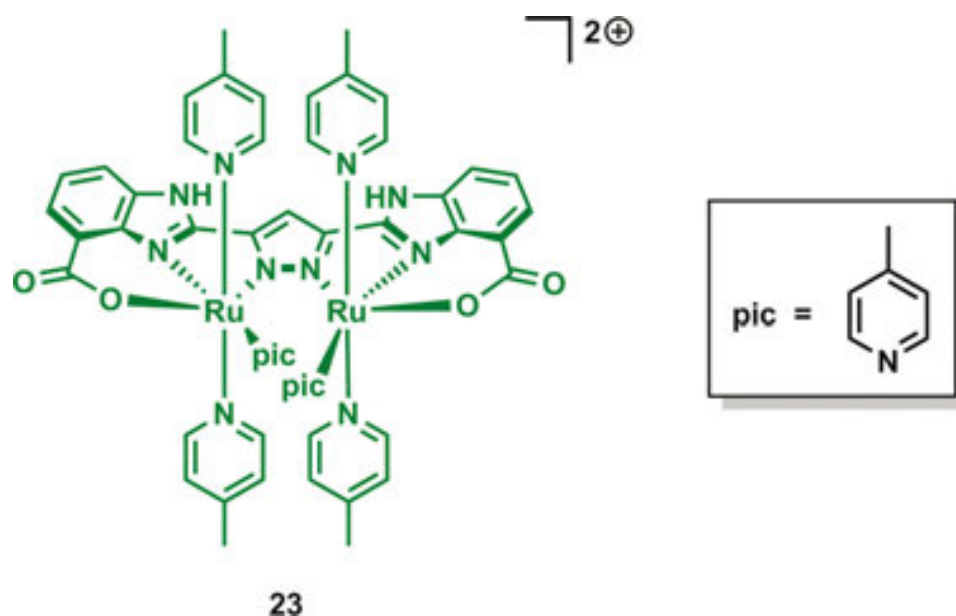


Figure 12. Structure of dinuclear ruthenium complex **23**.

Subsequent studies by the group of Sun and Åkermark focused on the dinuclear ruthenium complex **22**, which adopts a *cis* structure with phtalazine as the bridging unit (Figure 11) [53]. The electrochemical properties of the complex were studied by cyclic voltammetry in dry acetonitrile and exhibited two one-electron waves at 0.903 and 1.396 V vs. NHE. These were assigned to the redox processes $\text{Ru}_2^{\text{II,III}}/\text{Ru}_2^{\text{II,II}}$ and $\text{Ru}_2^{\text{III,III}}/\text{Ru}_2^{\text{II,III}}$, respectively. Despite the fact that the two ruthenium centers were oriented in a *cis* fashion, the redox potentials were higher than for ruthenium complex **21**, probably due to the strong electron donation from the aryl carbon bond to one of the ruthenium centers in complex **21**. The catalytic current for water oxidation for complex **22** takes place at onset potential of approximately 1.20 V vs. NHE in phosphate buffer at pH 7.2, which is lower than for complex **21**. TONs of 60, 420, 580, and TOFs of 0.1, 0.77, and 0.83 s^{-1} were obtained for the three photosensitizers **1–3**, respectively. Ruthenium complex **22** was shown to retain its catalytic activity upon the addition of photosensitizer

and sodium persulfate, and after the neutralization of pH, highlighting the stability of ruthenium complex **22** in the studied photochemical system.

A dinuclear ruthenium complex (**23**) for visible light-driven water oxidation was recently reported by the Åkermark group (Figure 12) [54]. Based on previous studies where a phenolate-based bridging ligand was utilized [55], it was envisioned that a ligand backbone consisting of a central pyrazole moiety would allow for the accommodation of two ruthenium centers. Employing an ancillary ligand scaffold consisting of a central pyrazole moiety and two benzimidazole units functionalized with carboxylate groups produced the dinuclear ruthenium complex **23** where the two metal centers are held in close proximity [54].

Several redox active species were observed in the electrochemical studies in phosphate buffer at pH 7.2. Oxidation peaks at potentials of approximately 0.05, 0.38, 0.70, 0.90, and 1.20 V vs. NHE were observed, with a catalytic current for water oxidation appeared at an onset potential of 1.20 V vs. NHE. The photochemical oxidation of water was initially carried out at pH 7.2, using $[\text{Ru}(\text{bpy})_2(\text{deeb})]^{2+}$ as photosensitizer. At a $3.0 \mu\text{M}$ catalyst concentration, the amount of evolved oxygen corresponded to a TON of 830. Lowering the pH led to a slight increase of the TON (890); however, a further decrease of the pH to 5.2 resulted in a substantial reduction in oxygen production, presumably due to the lower driving force. An increase of the pH to 8.2 also resulted in a significantly lower oxygen formation and was ascribed to the decomposition of the ruthenium-based photosensitizer [54]. A subsequent study has suggested that the designed ligand scaffold in dinuclear ruthenium complex **23** has a non-innocent behavior, in which the metal–ligand cooperation is an important feature during the four-electron oxidation of water and thus explains the observed catalytic efficiency of complex **23** [56].

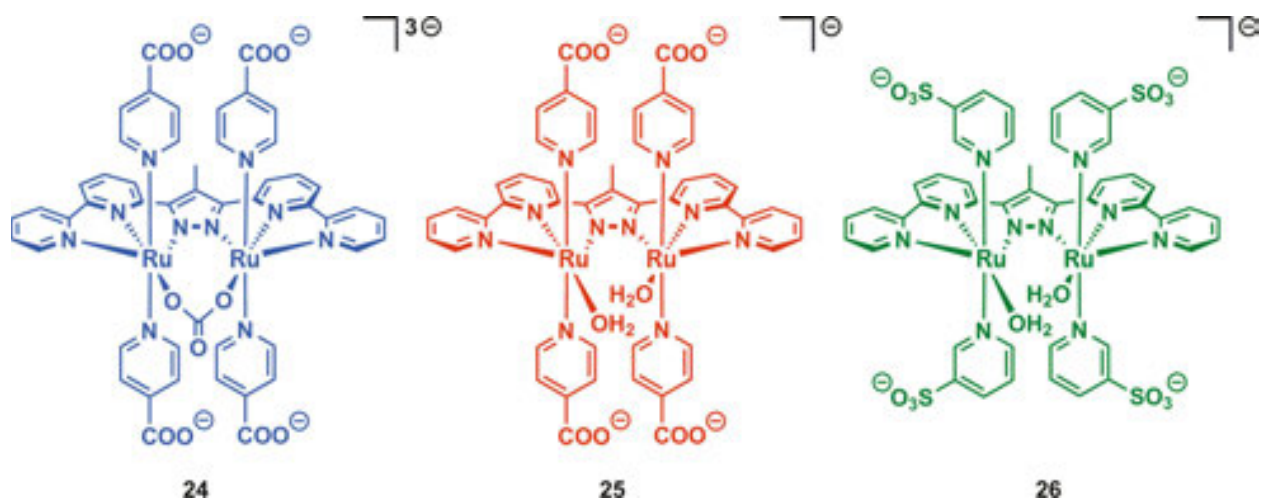


Figure 13. Dinuclear ruthenium complexes 24–26.

Llobet and coworkers reported a pyrazolate bpy-based dinuclear ruthenium complex **24** (Figure 13) [57]. The complex accommodates two ruthenium centers in a slightly distorted octahedral conformation. The metal ions are closely located within the pyrazole plane with a twisted carbonate bridging the two metals. The twisted conformation facilitates the exchange

of the carbonate with two water molecules in aqueous media, resulting in the formation of catalyst **25**. Electrochemical studies of complex **25** were conducted in phosphate buffer at pH 7. Two quasi-reversible redox processes at 0.59 and 0.88 V vs. NHE and the catalytic onset potential for water oxidation at 1.48 V vs. NHE could be observed, employing cyclic voltammetry.

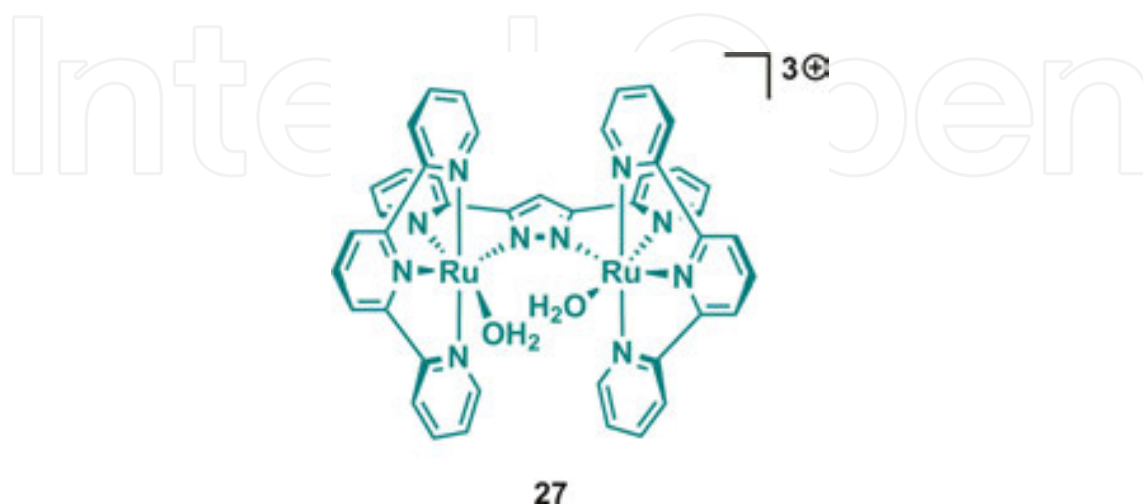


Figure 14. Depiction of the previously developed dinuclear ruthenium–pyrazole complex **27**.

The catalytic activity for light-driven water oxidation was measured at pH 7, using the $[\text{Ru}(\text{bpy})(\text{deeb})_2]^{2+}$ photosensitizer (**3**) together with sodium persulfate as the sacrificial electron acceptor. Sulfonate-based complex **26** gave rise to a TON of 2373 and a TOF of 11.1 s^{-1} in a single run. The experiments were repeated twice, resulting in a total TON of 5300. Complex **25** exhibited similar activity, producing a TON of >2300 and a TOF of 9.2 s^{-1} . The quantum yield (amount of molecular oxygen produced per absorbed photon) for complex **25**, under the above-mentioned conditions, reached 4.8% during 100 s of irradiation. The ligand design thus permits formation of a water soluble and oxidatively stable ruthenium complex, where the active catalyst reaches high TONs and TOFs for visible light-driven water oxidation [57].

The activity of **25** and **26** was compared with the previously reported complex **27** [58, 59] (Figure 14) under the exact same conditions, which further revealed the dramatic catalytic difference as catalyst **27** only yielded a TON of 67 and a TOF of 0.13 s^{-1} . An explanation for the lower activity of ruthenium complex **27** was assumed to be the high onset potential for water oxidation, occurring at 1.60 V vs. NHE, which is close to the redox potential provided by the $[\text{Ru}(\text{bpy})(\text{deeb})_2]^{2+}$ photosensitizer [57].

The catalytic efficiencies for the developed ruthenium-based complexes housing carboxylate-functionalized ligands and related complexes containing negatively charged ligand backbones highlight the robustness of these WOCs and suggest that such catalysts can be further heterogenized and applied onto photoanodes, which constitute an important part for the fabrication of devices for artificial photosynthesis.

3.2. Light-Driven Water Oxidation Catalyzed by Single-Site Ruthenium Complexes

Thummel and coworkers demonstrated that the ruthenium(II) polypyridyl complex **28** (Figure 15) was a viable catalyst for visible light-induced water oxidation [60]. The examination of the catalytic activity was carried out in a three-component homogeneous system containing $[\text{Ru}(\text{bpy})_3]^{2+}$ (**1**) as photosensitizer, persulfate as a sacrificial electron acceptor, and catalyst **28**. Under these conditions, complex **28** provided a TON of 103, a TOF of 0.12 s^{-1} , and a quantum yield of 9%. Mechanistic studies suggested that a unique proton-coupled low-energy pathway via a ruthenium(IV)-oxo intermediate takes place when using the mild photogenerated oxidant $[\text{Ru}(\text{bpy})_3]^{3+}$ (1.26 V vs. NHE) to drive water oxidation [60, 61].

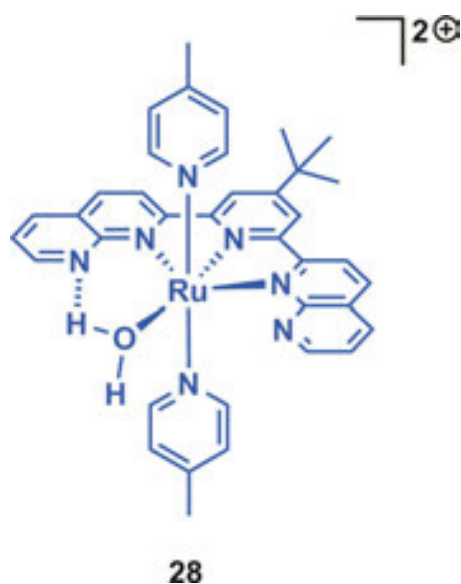


Figure 15. Structure of ruthenium(II) polypyridyl complex **28**.

Although a plethora of single-site ruthenium-based WOCs have been designed, only a handful has been shown to catalyze light-driven water oxidation. A majority of the ruthenium complexes that have been successful in driving water oxidation with visible light contain negatively charged ligand scaffolds, which are essential for lowering the redox potentials, allowing water oxidation to be driven by $[\text{Ru}(\text{bpy})_3]^{2+}$ -type photosensitizers.

The $[\text{Ru}(\text{bda})(\text{pic})_2(\text{OH}_2)]$ complex (**29**, Figure 16; bda = 2,2'-bipyridine-6,6'-dicarboxylic acid) is a rare example of a ruthenium complex containing a seven-coordinated ruthenium center [62]. The complex displays relatively low redox potentials, which makes it compatible with $[\text{Ru}(\text{bpy})_3]^{2+}$ -type photosensitizers. By using a three-component system consisting of ruthenium catalyst **29**, a $[\text{Ru}(\text{bpy})_3]^{2+}$ -type photosensitizer and sodium persulfate or $[\text{Co}(\text{NH}_3)_5\text{Cl}]\text{Cl}_2$ as sacrificial electron acceptors, molecular oxygen was generated [63, 64]. It was found that the catalytic system was rapidly deactivated due to the pH-dependent properties of ruthenium complex **29**. During the catalytic process, a rapid decrease of the pH of the reaction solution is observed, which affects the redox properties of catalyst **29** and decreases the catalytic activity. The authors found that adjusting the pH to 7.1 allowed for continued evolution of molecular

oxygen, highlighting that the observed fast deactivation is a result of the rapidly decreasing pH. The oxidative degradation of ruthenium complex **29** was also observed in both solution and the solid state under aerobic conditions. It could be established that complex **29** gradually decomposed via oxidative degradation of the axial picoline ligands, resulting in C(sp³)-H bond-oxidized ruthenium species.

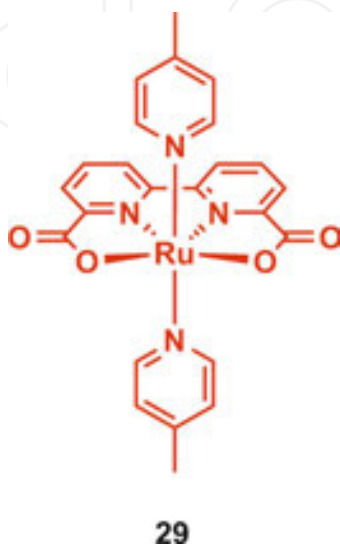


Figure 16. Structure of the [Ru(bda)(pic)₂(OH₂)] complex **29**.

The two structurally related ruthenium complexes **30** and **31** based on the tridentate 2,6-pyridinedicarboxylic acid ligand have also been studied for visible light-driven water oxidation (Figure 17) [65]. Despite their high structural resemblance, the two ruthenium complexes displayed significant difference in the activity in photochemical water oxidation. Using the [Ru(bpy)₂(deeb)]²⁺ (**2**)/S₂O₈²⁻ system, catalyst **30** triggered immediate oxygen evolution, producing a TON of 62 after 1 h of illumination. A linear dependence of the initial rate on complex **30** was observed using Ce^{IV} as chemical oxidant, implying that the catalyst most likely follows a mechanism involving the generation of a high-valent ruthenium-oxo species. Subsequent water nucleophilic attack on this species produces the key O–O bond, where additional oxidation events of the formed ruthenium-peroxo result in the liberation of molecular oxygen. In contrast to ruthenium complex **30**, complex **31** only generated a TON of 3.7, highlighting the dramatic difference in reactivity for the two ruthenium complexes. This difference was ascribed to the relative ease by which the complexes undergo picoline water ligand exchange, which was supported by mechanistic studies utilizing electrochemistry and ¹H NMR spectroscopy. In complex **30**, the equatorially bound picoline is rapidly replaced by a solvent water molecule, thus producing the catalytically important ruthenium-aqua species. By contrast, the ruthenium complex **31**, where bpy occupies the equatorial position, no such exchange was observed. These observations highlight that subtle changes in the ancillary ligand environments can dramatically affect the catalytic efficiencies of the studied ruthenium catalysts and are fundamental for designing WOCs with improved catalytic efficiencies.

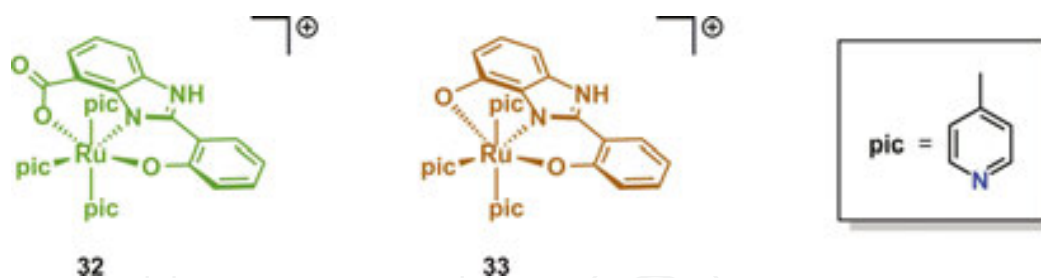


Figure 18. Molecular structures of ruthenium complexes 32 and 33.

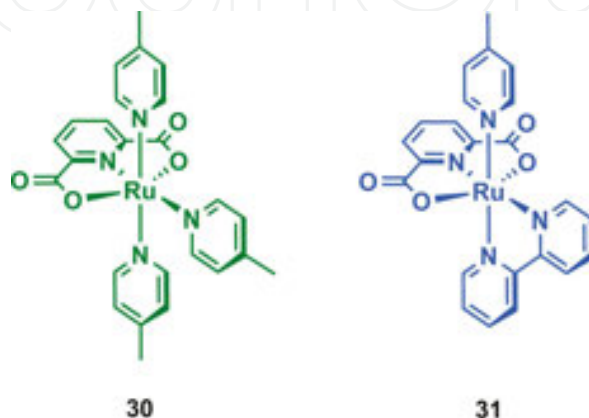


Figure 17. Depiction of the two structurally related ruthenium complexes 30 and 31.

Åkermark and coworkers have recently reported on the two single-site ruthenium complexes $[\text{Ru}(\text{Hhpbc})(\text{pic})_3]^+$ (**32**; H_3hpbc = 2-(2-hydroxyphenyl)-1*H*-benzo[*d*]imidazole-7-carboxylic acid) and $[\text{Ru}(\text{Hhpb})(\text{pic})_3]^+$ (**33**; H_3hpb = 2-(2-hydroxyphenyl)-1*H*-benzo[*d*]imidazol-7-ol) that contain two benzimidazole-based tridentate meridionally coordinating ligand frameworks (Figure 18) [66]. Inspired by nature, it was envisioned that the incorporation of negatively charged functional groups imidazole, phenol, and carboxylate, which have important functions in the natural photosynthetic system, would lower the redox potentials of the ruthenium complexes. Furthermore, inclusion of these potential proton transfer mediator motifs into the WOCs would also be expected to facilitate the simultaneous transfer of electrons and protons via proton-coupled electron transfer (PCET), which is crucial for avoiding charge buildup and high-energy intermediates. Catalytic experiments revealed that both ruthenium complexes were capable of mediating oxidation of water to molecular oxygen, both by use of pregenerated $[\text{Ru}(\text{bpy})_3]^{3+}$ as oxidant and driven by visible light. When using pregenerated $[\text{Ru}(\text{bpy})_3]^{3+}$, ruthenium complex **32** was able to generate a TON of ~ 4000 and TOF of $\sim 7 \text{ s}^{-1}$. In the photochemical setup, TONs of ~ 200 were obtained for the two ruthenium complexes **32** and **33** under neutral conditions using a three-component system consisting of $[\text{Ru}(\text{bpy})_2(\text{deeb})]^{2+}$ (**2**) as photosensitizer and persulfate as sacrificial electron acceptor. A recent study has suggested that O–O bond formation for the developed ruthenium complex **32** proceeds via a high-valent ruthenium(VI) species, where the capability of accessing this species is derived from the non-innocent ligand architecture (Figure 19) [67]. This cooperative catalytic involvement and the ability of accessing such high-valent species are intriguing and distinguish this ruthenium

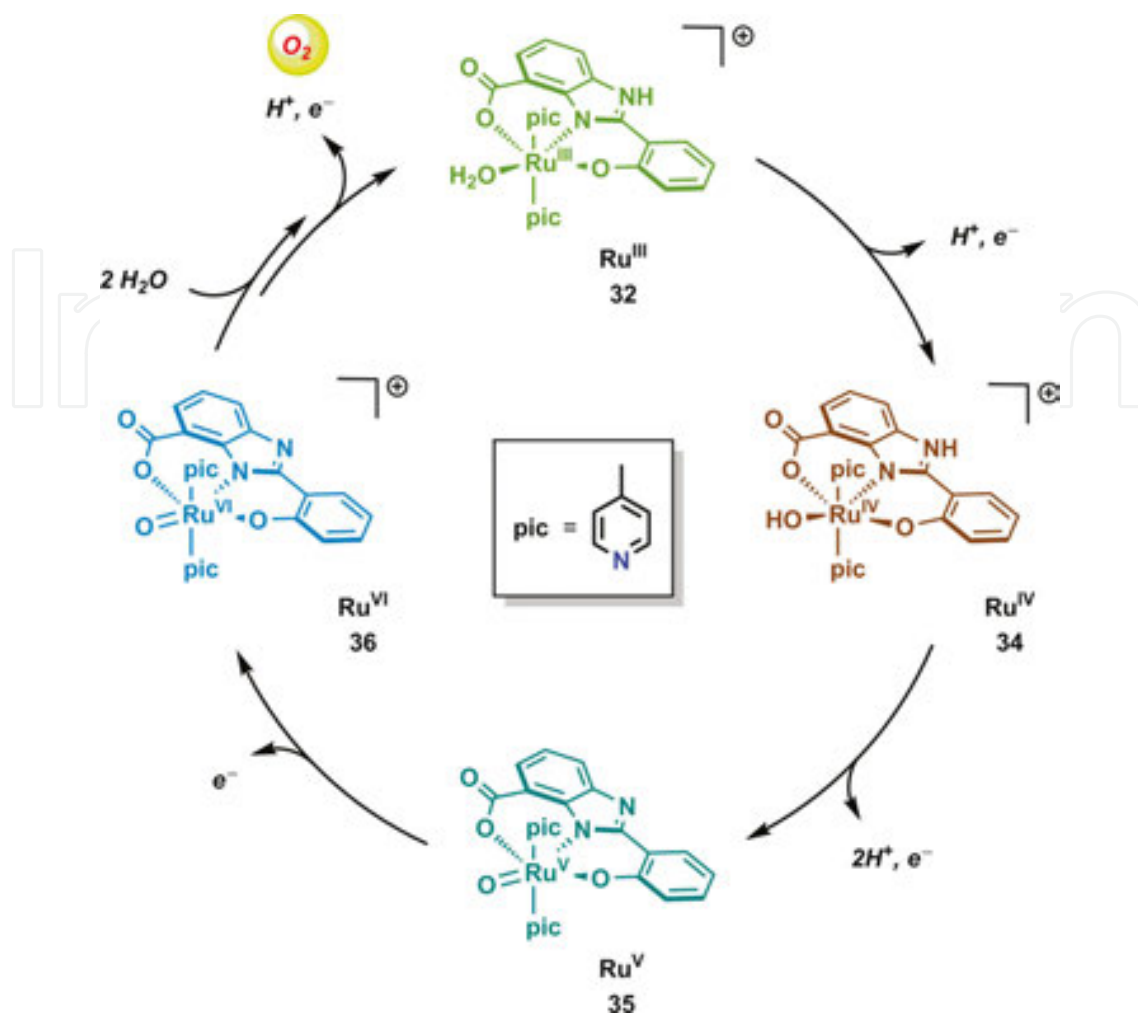


Figure 19. Proposed catalytic cycle for single-site ruthenium complex 32.

catalyst from the majority of previously reported complexes, which typically proceed via the generation of ruthenium(IV) or ruthenium(V) species as the catalytic key intermediate for O–O bond formation. This could thus provide the foundation for new pathways for the activation of small molecules such as water.

4. Molecular Chromophore–Catalyst Assemblies for Water Oxidation

Due to the progress that has been made in developing ruthenium-based catalysts for water oxidation, increased attention has recently been given to constructing supramolecular dyads where a photosensitizer and a WOC are covalently linked. These assemblies can subsequently be grafted onto solid electrodes, which would ultimately allow for visible light-driven water splitting [68, 69]. This chapter highlights some of the representative ruthenium-based assemblies and devices that have been constructed for photochemical and photoelectrochemical water oxidation.

4.1. Chromophore–Catalyst Assemblies for Homogeneous Water Oxidation

As a result of the synthetic complexity associated with linking a chromophore to a catalyst, there are only a limited number of examples of reported chromophore–catalyst assemblies. Here, the design of an appropriate linker is essential as these supramolecular assemblies have been shown to suffer from fast back electron transfer from the excited photosensitizer to the oxidized WOC entity [70].

Based on the promising results obtained with the $[\text{Ru}(\text{bda})(\text{pic})_2(\text{OH}_2)]$ complex **29** in visible light-driven water oxidation in the three-component system using sodium persulfate as sacrificial electron acceptor [63], Sun and coworkers decided to design supramolecular assemblies utilizing ruthenium complex **29** as the WOC unit [71]. For synthetic simplicity, the authors decided to introduce the photosensitizer moiety to the catalyst from its axial ligands. Two structurally different ruthenium-based photosensitizers were coupled to the WOC unit, which afforded the two ruthenium triads **37** and **38** (Figure 20). Due to the electron-rich bda ligand, the onset potential for water oxidation for triad **37** was observed at 0.96 V vs. NHE under neutral conditions, suggesting that the catalytic properties of the WOC unit are not significantly altered by linking it to the ruthenium photosensitizer. Furthermore, this also implies that water oxidation would be thermodynamically favorable. For ruthenium system **38**, the onset potential was observed at a slightly higher potential, yet still thermodynamically feasible. Photocatalytic experiments were performed in degassed phosphate buffer solutions, using sodium persulfate as the sacrificial electron acceptor. Upon irradiation with visible light ($\lambda > 400$ nm), triad **37** rapidly generated molecular oxygen with a TOF of 0.078 s^{-1} . Control experiments confirmed that light, assembly, and electron acceptor were all required to achieve the evolution of molecular oxygen. A vital question was whether assembly **37** would be more effective than the corresponding separate system consisting of $[\text{Ru}(\text{bda})(\text{pic})_2]$ (**29**), $[\text{Ru}(\text{bpy})_3]^{2+}$ (**1**), and sodium persulfate. This comparison revealed an almost fivefold difference in activity, where assembly **37** provided a TON of 38 vs. a TON of 8 for the non-coupled system. The degradation pathway for the coupled system **37** was also addressed by the use of mass spectrometry, which revealed a correlation between slow ligand dissociation of one of the two axial photosensitizer units of the assembly and the decrease in water oxidation activity over time. In contrast to ruthenium triad **37**, no oxygen was generated when using **38**. This dramatic difference in reactivity was attributed to the significantly shorter excited state lifetime of the $[\text{Ru}(\text{tpy})_2]^{2+}$ -units (tpy = 2,2';6',2''-terpyridine) in assembly **38** relative to that of the $[\text{Ru}(\text{bpy})_3]^{2+}$ -units of **37**. Although system **38** proved to be inactive, this work highlights that supramolecular assemblies for visible light-driven water oxidation can be constructed by matching two light-harvesting sites and a catalytic WOC unit. Subsequent studies on ruthenium triad **39** (Figure 20) established that this produced a significantly higher TON of 200 when driven by visible light [72]. Here, photocatalytic experiments in combination with time-resolved spectroscopy showed that the linked catalyst in its ruthenium(II) state rapidly quenches the photosensitizer, predominantly by energy transfer. The higher photostability of assembly **39** compared to the three component system was attributed to kinetic stabilization by rapid photosensitizer regeneration. A supramolecular assembly where $[\text{Ru}(\text{bda})(\text{pic})_2]$ complex (**29**) was incorporated into a cyclodextrin-modified $[\text{Ru}(\text{bpy})_3]^{2+}$ -type photosensitizer

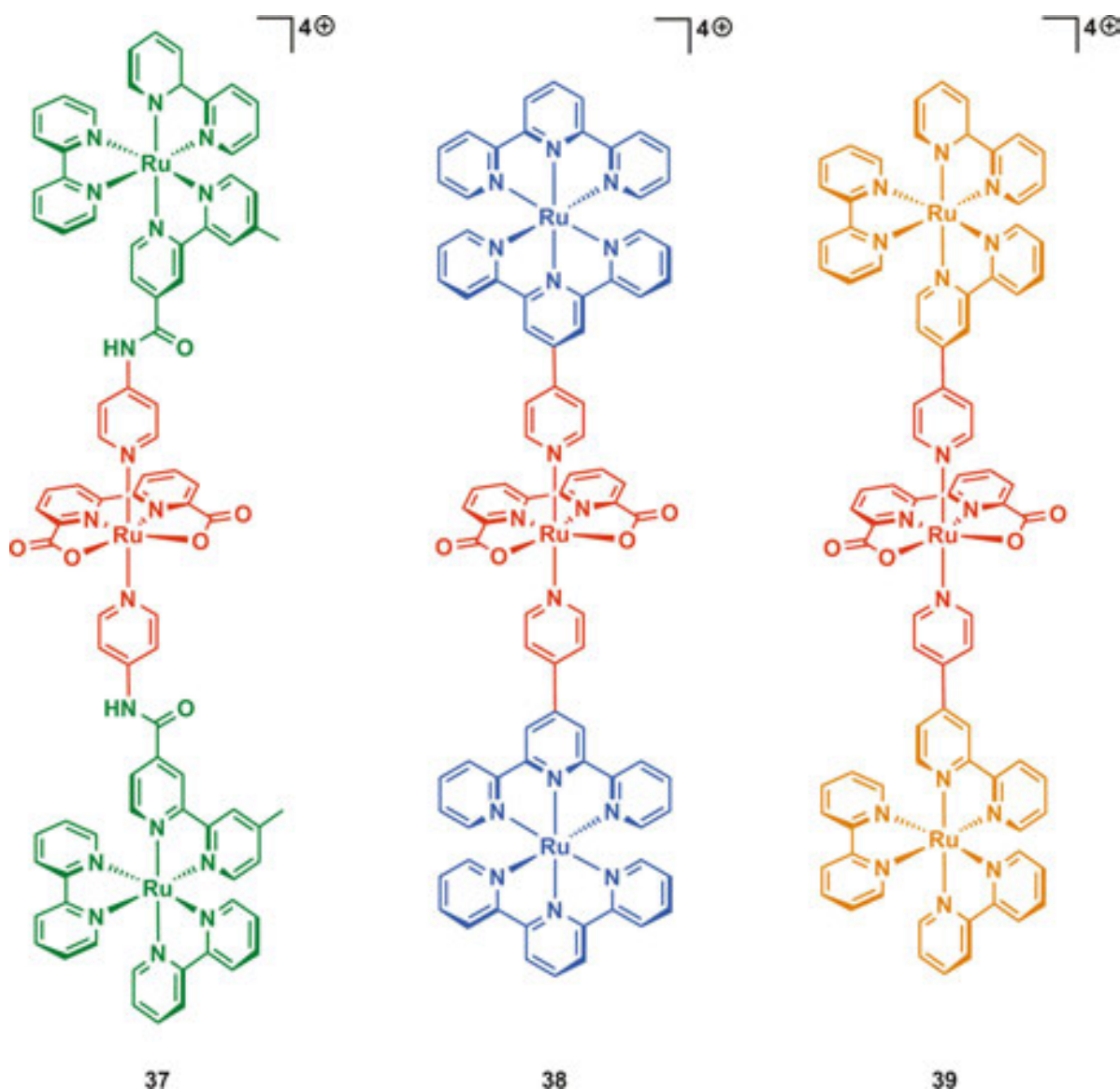


Figure 20. Depiction of the molecular assemblies 37–39 based on the $[\text{Ru}(\text{bda})(\text{pic})_2(\text{OH}_2)]$ complex 29.

has recently also been developed for visible light-driven water oxidation employing persulfate as the sacrificial electron acceptor [73]. A remarkable quantum efficiency of 84% was determined for the host–guest adduct under visible light irradiation, which is nearly one order of magnitude higher than that of non-interaction system, indicating that noncovalent incorporation of photosensitizer and catalyst entities is an appealing approach for realizing efficient conversion of solar energy into fuels.

4.2. Surface-Bound Chromophore–Catalyst Assemblies

Dye-sensitized photoelectrochemical cells (DSPECs) for water splitting consist of a photoanode, which is connected via an external circuit to a cathode. A characteristic feature is also the use of a membrane, which is supposed to prevent mixing of the generated gaseous products. The membrane should also be permeable to proton diffusion, in order to allow

equilibration between the cell compartments. In a majority of water-splitting cells based on TiO_2 , an external bias of ~ 0.2 V is needed for efficient reduction of the produced protons to hydrogen gas and maximize water splitting [74–76].

At the core of DSPECs for water splitting, is the chromophore–catalyst assembly that is supposed to mediate water oxidation. Important characteristics of this are 1) robust anchoring to the electrode surface, which also allows electron transfer events to take place through electronic orbital coupling, 2) chromophores that display broad absorption of visible light that 3) upon excitation undergo electron injection into the conduction band of the photoanode, and 4) a stable and efficient WOC entity, having catalytic rates that exceed the rate of solar insolation. It is also essential that the oxidized chromophore is rapidly reduced by the WOC. The ruthenium-based chromophores are in general highly unstable in their oxidized state, which facilitates degradation via nucleophilic attack of water or buffer anions, and back electron transfer events can occur from the semiconductor, thus regenerating the reduced state of the chromophore resulting in low quantum yields [74–77].

The covalent attachment of chromophores and/or WOC to the high surface area of the oxide-based semiconductor is a critical feature that needs to be targeted in order to prevent detachment of the molecular entity from the oxide surface. A variety of strategies for anchoring molecular chromophores, WOCs, and chromophore–catalyst assemblies to oxide surfaces have therefore been evaluated. Reported examples include the use of acetylacetonates [78], alkoxides [79], hydroxamates [80], and siloxanes [81]. However, the most widely used functional groups are carboxylic ($-\text{COOH}$) and phosphonic acid ($-\text{PO}_3\text{H}_2$) derivatives. Carboxylic acids are the most frequently used linking groups in dye-sensitized solar cells (DSSCs) where they provide strong electronic coupling for ultrafast electron injection from the excited state of the dye. Under nonaqueous conditions, surface detachment is not a limiting factor; however, photoanodes for water splitting operate in aqueous solutions, thus causing irreversible hydrolysis of the covalently attached molecular scaffold and limiting the lifetime of the assemblies. An attractive alternative is the use of phosphonate linkers (Figure 21), which provide more robust surface binding and are typically resistant to hydrolysis/desorption at $\text{pH} > 5$ with added buffer bases [82–85].

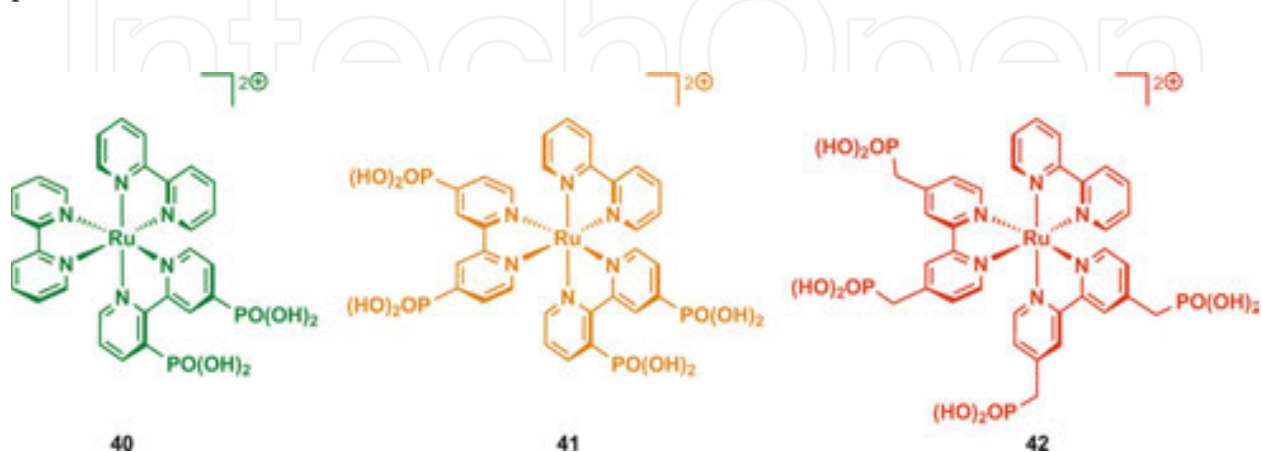


Figure 21. Structures of phosphonate-derivatized ruthenium(II) photosensitizers 40–42.

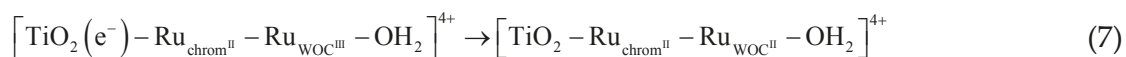


Figure 22. Structure of chromophore–catalyst assembly **43**.

It has been suggested that the presence of molecular oxygen facilitates the photodesorption of phosphonate-linked dyes in aqueous solutions, presumably due to the formation of superoxide ions through back electron transfer from TiO_2 . This problem can partially be circumvented by constructing chromophores with multiple ligating phosphonate units. However, the electron injection ability of the chromophores decreases with increasing number of phosphonate groups, highlighting that additional work on designing chromophores for surface stabilization is needed [86].

From the aforementioned discussion, it is apparent that fast electron transfer between the WOC and the oxidized photosensitizer is vital for achieving efficient and robust water-splitting cells. Recent work has shown that the use of phosphonate linkages has limited impact on the reactivity or properties of surface-bound assemblies, thus maintaining the reactivity observed for the homogeneous system [87].

Meyer and coworkers have designed several chromophore–catalyst assemblies that upon attachment to oxide surfaces are able to mediate electrocatalytic water oxidation [88–90]. For the chromophore–catalyst **43** depicted in Figure 22, an amide-based linker ligand was utilized to couple the WOC unit to the chromophore. The synthetically flexible saturated amide bridge ligand was designed to enable long-lived charge-separated states. Interfacial dynamics analysis of dyad **43** by nanosecond transient absorption measurements revealed that upon excitation of the ruthenium chromophore, rapid electron injection into TiO_2 occurred, which was followed by intra-assembly electron transfer from the ruthenium–WOC unit to the oxidized chromophore. This process takes place on the subnanosecond timescale and was followed by microsecond–millisecond back electron transfer from the semiconductor to the oxidized WOC entity (Eq. 7) [91].



An attractive approach for constructing catalytic assemblies for light-driven water splitting involves the layer-by-layer addition of a chromophore followed by a catalyst overlayer. Such co-loading strategies allow for straightforward, and potentially practical, approaches for surface attachment and are considered to be general and simple alternatives for producing functioning DSPEC photoanodes [92–94].

An example of such an approach can be seen in Sun and coworkers' photoanode where a derivative of a previously developed ruthenium-based WOC **29** (**44**) was immobilized together with a molecular ruthenium photosensitizer (**45**) on nanostructured TiO₂ particles on fluorine-doped tin oxide (FTO) conducting glass (Figure 23) [95]. Electrochemical measurements revealed an irreversible oxidation peak at $E_{\text{pa}} = 1.40$ V vs. NHE, which was assigned to the Ru^{III}/Ru^{II} redox couple of photosensitizer **45**. A redox process at $E_{1/2} = 0.71$ V vs. NHE, assigned to the Ru^{III}/Ru^{II} redox couple of catalyst **44**, was also observed, which was followed by a catalytic wave with an onset potential of 1.14 V vs. NHE corresponding to the oxidation of water. From the electrochemical experiments, it could also be established that the ratio of photosensitizer/catalyst was 3:1. A three-electrode PEC cell was constructed using the synthesized photoanode as working electrode, Ag/AgCl as the reference electrode and platinum wire as the cathode for visible light-driven ($\lambda > 400$ nm) water splitting. An external bias of 0.2 V vs. NHE was applied in order to allow for efficient electron transfer. The incident photo-to-current conversion efficiency (IPCE) spectrum of the constructed PEC cell was also measured and showed a maximum IPCE value of 14% at ~450 nm, which corresponds well with the UV–vis absorption spectrum of the developed photoanode. After ~500 s of visible light illumination, the amount of molecular oxygen and hydrogen gas produced was calculated. A TON of almost 500 and a TOF of 1.0 s⁻¹ (based on catalyst **44**) were calculated with Faradaic efficiencies of 83% and 74%, respectively, highlighting the efficiency of the fabricated PEC cell. Subsequent work has focused on employing different anchoring groups on the WOC entity (Figure 24) and includes the use of the phosphonate-functionalized catalyst **46** [96], the acrylate-functionalized catalyst **47** [97], and the vinyl-functionalized catalyst **48** [98, 99], which was used for electrochemical polymerization onto nanoporous TiO₂ and Fe₂O₃ films, and a ruthenium-based catalyst containing a long carbon chain in combination with poly(methyl methacrylate) as the auxiliary material [100].

5. Conclusions

As a consequence of the depleting energy resources and the increasing need for energy, modern society faces a daunting task of realizing sustainable, carbon-neutral alternatives. In this context, the development of solar-to-fuel conversion technologies by mimicking the natural photosynthetic apparatus is considered as an attractive solution. While significant effort has been devoted to designing artificial systems for solar energy conversion, replicating the essential functions of natural photosynthesis has proved to be intricate.

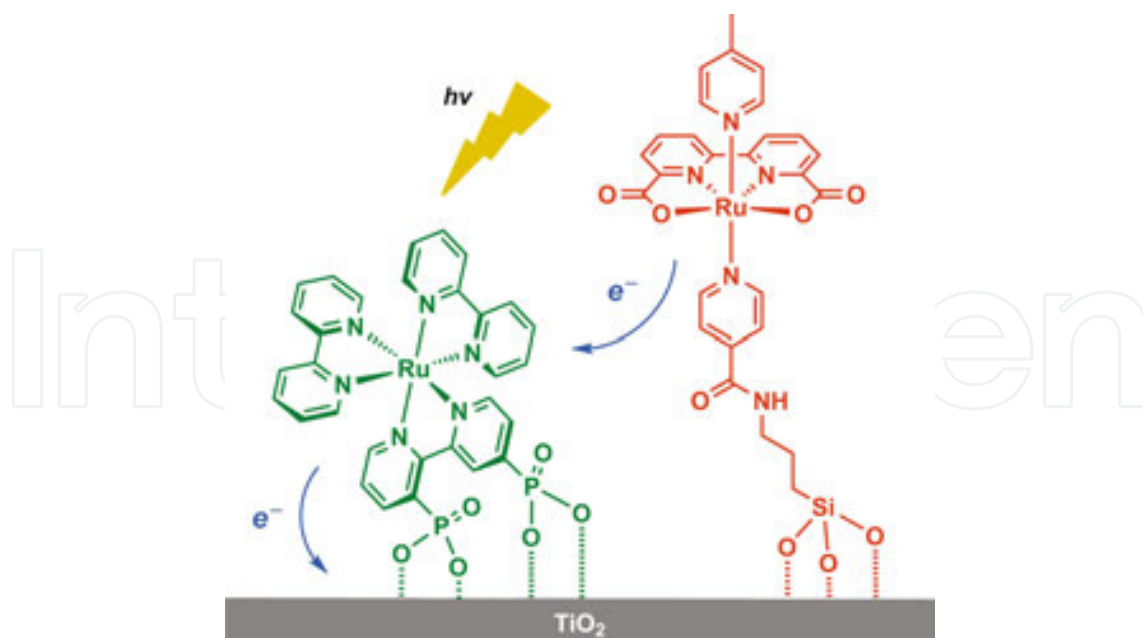


Figure 23. Co-immobilization of ruthenium WOC 44 and ruthenium photosensitizer 45 onto nanostructured TiO₂ particles for visible light-driven water splitting.

An essential component in light-harvesting devices is a catalyst that is able to oxidize water to molecular oxygen, thereby providing the necessary reducing equivalents for reduction of protons to hydrogen gas. Photo-induced charge separation and buildup of multiple redox equivalents is also an essential part of solar-to-fuel conversion schemes. The catalysts reviewed here represent the state of the art and are hence capable of mediating homogeneous light-driven water oxidation through the accumulation of multiple redox equivalents at the catalytic center. The envisioned assemblies for water splitting consist of three parts—a chromophore, a catalyst for water oxidation, and a semiconductor—and have mainly been developed

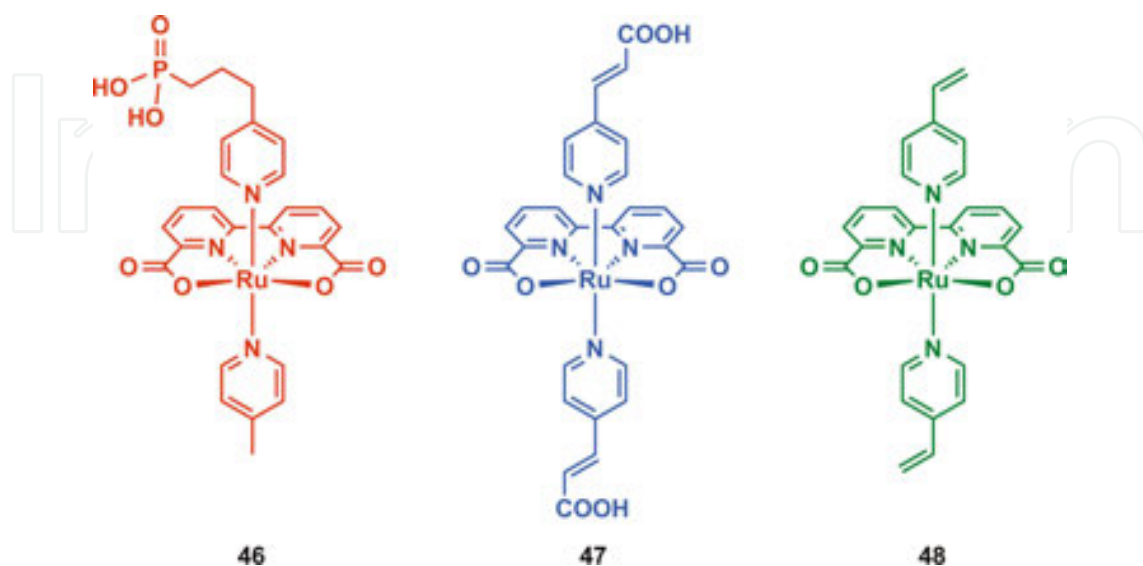


Figure 24. Ruthenium-based catalysts 46–48 employed for fabrication of photoanodes.

separately. The current limitation of these assemblies is related to the inefficient coupling of the individual catalytic events, which is necessary for the development of efficient artificial photosynthetic systems.

Considerable progress has been made during the last decade in constructing photochemical cells capable of splitting water. However, the fundamental aspects, including their synthesis, their long-term durability, and the mechanistic understanding, are far from resolved and are of significant concern. Further elaboration and assembling of all of the integral components through cooperative interplay will certainly continue, thereby realizing efficient artificial photosynthesis in a not too distant future.

Acknowledgements

Financial support from the Swedish Research Council (637-2013-7314, 2015-04995 and 621-2013-4872), Swedish Foundation for Strategic Research, Stiftelsen Olle Engkvist Byggmästare, the Knut and Alice Wallenberg Foundation, and the Carl Trygger Foundation is gratefully acknowledged.

Author details

Markus D. Kärkäs*, Tanja M. Laine, Eric V. Johnston* and Björn Åkermark*

*Address all correspondence to: markus.karkas@su.se (M. D. K.)

*Address all correspondence to: eric.johnston@su.se (E. V. J.)

*Address all correspondence to: bjorn.akermark@su.se (B. Å.)

Department of Organic Chemistry, Arrhenius Laboratory, Stockholm University, Stockholm, Sweden.

References

- [1] Chow, J., Kopp, R. J., Portney, P. R. Energy resources and global development. *Science*, 2003. 302: pp. 1528–1531. doi: 10.1126/science.1091939
- [2] Lewis, N. S., Nocera, D. G. Powering the planet: Chemical challenges in solar energy utilization. *Proc. Natl. Acad. Sci. U. S. A.*, 2006. 103: pp. 15729–15735. doi: 10.1073/pnas.0603395103

- [3] Gray, H. B. Powering the planet with solar fuel. *Nature Chem*, 2009. 1: pp. 7. doi: 10.1038/nchem.141
- [4] Cho, A. Energy's tricky tradeoffs. *Science*, 2010. 329: pp. 786–787. doi: 10.1126/science.329.5993.786
- [5] Han, Z., Eisenberg, R. Fuel from water: The photochemical generation of hydrogen from water. *Acc. Chem. Res*, 2014. 47: pp. 2537–2544. doi: 10.1021/ar5001605
- [6] Pagliaro, M., Konstandopoulos, A. G., Ciriminna, R., Palmisano, G. Solar hydrogen: Fuel of the near future. *Energy Environ. Sci*, 2010. 3: pp. 279–287. doi: 10.1039/B923793N
- [7] Meyer, T. J. Chemical approaches to artificial photosynthesis. *Acc. Chem. Res*, 1989. 22: pp. 163–170. doi: 10.1021/ar00161a001
- [8] Suga, M., Akita, F., Hirata, K., Ueno, G., Murakami, H., Nakajima, Y., Shimizu, T., Yamashita, K., Yamamoto, M., Ago, H., Shen, J.-R. Native structure of photosystem II at 1.95 Å resolution viewed by femtosecond X-ray pulses. *Nature*, 2015. 517: pp. 99–103. doi: 10.1038/nature13991
- [9] Wydrzynski, T. J., Satoh, K. (eds.). *Photosystem II: The Light-Driven Water Plastoquinone Oxidoreductase*. Dordrecht, The Netherlands: Springer. 2005. doi: 10.1007/1-4020-4254-X
- [10] Barber, J., Tran, P. D. From natural to artificial photosynthesis. *J. R. Soc. Interface*, 2013. 10: pp. 20120984. doi: 10.1098/rsif.2012.0984
- [11] Sun, L., Hammarström, L., Åkermark, B., Styring, S. Towards artificial photosynthesis: Ruthenium-manganese chemistry for energy production. *Chem. Soc. Rev*, 2001. 30: pp. 36–49. doi: 10.1039/A801490F
- [12] Barber, J. Photosynthetic energy conversion: Natural and artificial. *Chem. Soc. Rev*, 2009. 38: pp. 185–196. doi: 10.1039/B802262N
- [13] McDaniel, N. D., Bernhard, S. Solar fuels: Thermodynamics, candidates, tactics, and figures of merit. *Dalton Trans*, 2010. 39: pp. 10021–10030. doi: 10.1039/C0DT00454E
- [14] Fujishima, A., Honda, K. Electrochemical photolysis of water at a semiconductor electrode. *Nature*, 1972. 238: pp. 37–38. doi: 10.1038/238037a0
- [15] Swierk, J. R., Mallouk, T. E. Design and development of photoanodes for water-splitting dye-sensitized photoelectrochemical cells. *Chem. Soc. Rev*, 2013. 42: pp. 2357–2387. doi: 10.1039/c2cs35246j
- [16] Knör, G. Recent progress in homogeneous multielectron transfer photocatalysis and artificial photosynthetic solar energy conversion. *Coord. Chem. Rev*, 2015. 304–305: pp. 102–108. doi: 10.1016/j.ccr.2014.09.013

- [17] Kärkäs, M. D., Johnston, E. V., Verho, O., Åkermark, B. Artificial photosynthesis: From nanosecond electron transfer to catalytic water oxidation. *Acc. Chem. Res*, 2014. 47: pp. 100–111. doi: 10.1021/ar400076j
- [18] Alstrum-Acevedo, J. H., Brennaman, M. K., Meyer, T. J. Chemical approaches to artificial photosynthesis. 2. *Inorg. Chem*, 2005. 44: pp. 6802–6827. doi: 10.1021/ic050904r
- [19] Gust, D., Moore, T. A., Moore, A. L. Mimicking photosynthetic solar energy transduction. *Acc. Chem. Res*, 2001. 34: pp. 40–48. doi: DOI: 10.1021/ar9801301
- [20] Knör, G. Artificial enzyme catalysis controlled and driven by light. *Chem. Eur. J*, 2009. 15: pp. 568–578. doi: 10.1002/chem.200801179
- [21] Knör, G., Monkowius, U. Photosensitization and photocatalysis in bioinorganic, bioorganometallic and biomimetic systems. *Adv. Inorg. Chem*, 2011. 63: pp. 235–289. doi: 10.1016/B978-0-12-385904-4.00005-6
- [22] Marcus, R. A., Sutin, N. Electron transfers in chemistry and biology. *Biochim. Biophys. Acta*, 1985. 811: pp. 265–322. doi: 10.1016/0304-4173(85)90014-X
- [23] Gust, D., Moore, T. A., Moore, A. L. Molecular mimicry of photosynthetic energy and electron transfer. *Acc. Chem. Res*, 1993. 26: pp. 198–205. doi: DOI: 10.1021/ar00028a010
- [24] Kalyanasundaram, K. Photophysics, photochemistry and solar energy conversion with tris(bipyridyl)ruthenium(II) and its analogues. *Coord. Chem. Rev*, 1982. 46: pp. 159–244. doi: 10.1016/0010-8545(82)85003-0
- [25] Juris, A., Balzani, V., Barigelletti, F., Campagna, S., Belser, P., von Zelewsky, A. Ru(II) polypyridine complexes: photophysics, photochemistry, electrochemistry, and chemiluminescence. *Coord. Chem. Rev*, 1988. 84: pp. 85–277. doi: 10.1016/0010-8545(88)80032-8
- [26] Campagna, S., Puntoriero, F., Nastasi, F., Bergamini, G., Balzani, V. Photochemistry and photophysics of coordination compounds: Ruthenium. *Top. Curr. Chem*, 2007. 280: pp. 117–214. doi: 10.1007/128_2007_133
- [27] Gau, B. C., Chen, H., Zhang, Y., Gross, M. L. Sulfate radical anion as a new reagent for fast photochemical oxidation of proteins. *Anal. Chem*, 2010. 82: pp. 7821–7827. doi: 10.1021/ac101760y
- [28] Bolletta, F., Juris, A., Maestri, M., Sandrini, D. Quantum yield of formation of the lowest excited state of Ru(bpy)₃²⁺ and Ru(phen)₃²⁺. *Inorg. Chim. Acta*, 1980. 44: pp. L175–L176. doi: 10.1016/S0020-1693(00)90993-9
- [29] Kärkäs, M. D., Verho, O., Johnston, E. V., Åkermark, B. Artificial photosynthesis: Molecular systems for catalytic water oxidation. *Chem. Rev*, 2014. 114: pp. 11863–12001. doi: 10.1021/cr400572f
- [30] Blakemore, J. D., Crabtree, R. H., Brudvig, G. W. Molecular catalysts for water oxidation. *Chem. Rev*, 2015. 115: pp. 12974–13005. doi: 10.1021/acs.chemrev.5b00122

- [31] Sala, X., Maji, S., Bofill, R., García-Antón, J., Escriche, L., Llobet, A. Molecular water oxidation mechanisms followed by transition metals: State of the art. *Acc. Chem. Res.*, 2014. 47: pp. 504–516. doi: 10.1021/ar400169p
- [32] Das, B., Orthaber, A., Ott, S., Thapper, A. Water oxidation catalysed by a mononuclear Co^{II} polypyridine complex; possible reaction intermediates and the role of the chloride ligand. *Chem. Commun.*, 2015. 51: pp. 13074–13077. doi: 10.1039/c5cc04148a
- [33] Nakazono, T., Parent, A. R., Sakai, K. Cobalt porphyrins as homogeneous catalysts for water oxidation. *Chem. Commun.*, 2013. 49: pp. 6325–6327. doi: 10.1039/c3cc43031f
- [34] Leung, C.-F., Ng, S.-M., Ko, C.-C., Man, W.-L., Wu, J., Chen, L., Lau, T.-C. A cobalt(II) quaterpyridine complex as a visible light-driven catalyst for both water oxidation and reduction. *Energy Environ. Sci.*, 2012. 5: pp. 7903–7907. doi: 10.1039/C2EE21840B
- [35] Wang, H.-Y., Mijangos, E., Ott, S., Thapper, A. Water oxidation catalyzed by a dinuclear cobalt-polypyridine complex. *Angew. Chem. Int. Ed.*, 2014. 53: pp. 14499–14502. doi: 10.1002/anie.201406540
- [36] Barnett, S. M., Goldberg, K. I., Mayer, J. M. A soluble copper-bipyridine water-oxidation electrocatalyst. *Nature Chem.*, 2012. 4: pp. 498–502. doi: 10.1038/nchem.1350
- [37] Garrido-Barros, P., Funes-Ardoiz, I., Drouet, S., Benet-Buchholz, J., Maseras, F., Llobet, A. Redox non-innocent ligand controls water oxidation overpotential in a new family of mononuclear Cu-based efficient catalysts. *J. Am. Chem. Soc.*, 2015. 137: pp. 6758–6761. doi: 10.1021/jacs.5b03977
- [38] Su, X.-J., Gao, M., Jiao, L., Liao, R.-Z., Siegbahn, P. E. M., Cheng, J.-P., Zhang, M.-T. Electrocatalytic water oxidation by a dinuclear copper complex in a neutral aqueous solution. *Angew. Chem. Int. Ed.*, 2015. 54: pp. 4909–4914. doi: 10.1002/anie.201411625
- [39] Coggins, M. K., Zhang, M.-T., Vannucci, A. K., Dares, C. J., Meyer, T. J. Electrocatalytic water oxidation by a monomeric amidate-ligated Fe(III)-aqua complex. *J. Am. Chem. Soc.*, 2014. 136: pp. 5531–5534. doi: 10.1021/ja412822u
- [40] Najafpour, M. M., Moghaddam, A. N., Sedigh, D. J., Hołyńska, M. A dinuclear iron complex with a single oxo bridge as an efficient water-oxidizing catalyst in the presence of cerium(IV) ammonium nitrate: New findings and current controversies. *Catal. Sci. Technol.*, 2014. 4: pp. 30–33. doi: 10.1039/C3CY00644A
- [41] Wickramasinghe, L. D., Zhou, R., Zong, R., Vo, P., Gagnon, K. J., Thummel, R. P. Iron complexes of square planar tetradentate polypyridyl-type ligands as catalysts for water oxidation. *J. Am. Chem. Soc.*, 2015. 137: pp. 13260–13263. doi: 10.1021/jacs.5b08856
- [42] Codolà, Z., Gómez, L., Kleespies, S. T., Que, L. Jr., Costas, M., Lloret-Fillol, J. Evidence for an oxygen evolving iron-oxo-cerium intermediate in iron-catalysed water oxidation. *Nature Commun.*, 2015. 6: 5865. doi: 10.1038/ncomms6865

- [43] Limburg, J., Vrettos, J. S., Liabe-Sands, L. M., Rheingold, A. L., Crabtree, R. H., Brudvig, G. W. A functional model for O–O bond formation by the O₂-evolving complex in photosystem II. *Science*, 1999. 283: pp. 1524–1527. doi: 10.1126/science.283.5407.1524
- [44] Karlsson, E. A., Lee, B.-L., Åkermark, T., Johnston, E. V., Kärkäs, M. D., Sun, J., Hansson, Ö., Bäckvall, J.-E., Åkermark, B. Photosensitized water oxidation by use of a bioinspired manganese catalyst. *Angew. Chem. Int. Ed*, 2011. 50: pp. 11715–11718. doi: 10.1002/anie.201104355
- [45] Liao, R.-Z., Kärkäs, M. D., Lee, B.-L., Åkermark, B., Siegbahn, P. E. M. Photosystem II like water oxidation mechanism in a bioinspired tetranuclear manganese complex. *Inorg. Chem*, 2015. 54: pp. 342–351. doi: 10.1021/ic5024983
- [46] Lee, W.-T., Muñoz, S. B. III., Dickie, D. A., Smith, J. M. Ligand modification transforms a catalase mimic into a water oxidation catalyst. *Angew. Chem. Int. Ed*, 2014. 53: pp. 9856–9859. doi: 10.1002/anie.201402407
- [47] Gao, Y., Åkermark, T., Liu, J., Sun, L., Åkermark, B. Nucleophilic attack of hydroxide on a Mn^V oxo vomplex: A model of the O–O bond formation in the oxygen evolving complex of photosystem II. *J. Am. Chem. Soc*, 2009. 131: pp. 8726–8727. doi: 10.1021/ja901139r
- [48] Gersten, S. W., Samuels, G. J., Meyer, T. J. Catalytic oxidation of water by an oxo-bridged ruthenium dimer. *J. Am. Chem. Soc*, 1982. 104: pp. 4029–4030. doi: 10.1021/ja00378a053
- [49] Gilbert, J. A., Eggleston, D. S., Murphy, W. R. Jr., Geselowitz, D. A., Gersten, S. W., Hodgson, D. J., Meyer, T. J. Structure and redox properties of the water-oxidation catalyst [(bpy)₂(OH₂)RuORu(OH₂)(bpy)₂]⁴⁺. *J. Am. Chem. Soc*, 1985. 107: pp. 3855–3864. doi: 10.1021/ja00299a017
- [50] Rotzinger, F. P., Munavalli, S., Comte, P., Hurst, J. K., Grätzel, M., Pern, F. J., Frank, A. J. A molecular water-oxidation catalyst derived from ruthenium diaqua bis(2,2'-bipyridyl-5,5'-dicarboxylic acid). *J. Am. Chem. Soc*, 1987. 109: pp. 6619–6626. doi: 10.1021/ja00256a010
- [51] Xu, Y., Åkermark, T., Gyollai, V., Zou, D., Eriksson, L., Duan, L., Zhang, R., Åkermark, B., Sun, L. A new dinuclear ruthenium complex as an efficient water oxidation catalyst. *Inorg. Chem*, 2009. 48: pp. 2717–2719. doi: 10.1021/ic802052u
- [52] Xu, Y., Duan, L., Tong, L., Åkermark, B., Sun, L. Visible light-driven water oxidation catalyzed by a highly efficient dinuclear ruthenium complex. *Chem. Commun*, 2010. 46: pp. 6506–6508. doi: 10.1039/C0CC01250E
- [53] Xu, Y., Fischer, A., Duan, L., Tong, L., Gabrielsson, E., Åkermark, B., Sun, L. Chemical and light-driven oxidation of water catalyzed by an efficient dinuclear ruthenium complex. *Angew. Chem. Int. Ed*, 2010. 49: pp. 8934–8937. doi: 10.1002/anie.201004278
- [54] Laine, T. M., Kärkäs, M. D., Liao, R.-Z., Åkermark, T., Lee, B.-L., Karlsson, E. A., Siegbahn, P. E. M., Åkermark, B. Efficient photochemical water oxidation by a dinuclear

- molecular ruthenium complex. *Chem. Commun*, 2015. 51: pp. 1862–1865. doi: 10.1039/C4CC08606F
- [55] Kärkäs, M. D., Johnston, E. V., Karlsson, E. A., Lee, B.-L., Åkermark, T., Shariatgorji, M., Ilag, L., Hansson, Ö., Bäckvall, J.-E., Åkermark, B. Light-induced water oxidation by a Ru complex containing a bio-inspired ligand. *Chem. Eur. J*, 2011. 17: pp. 7953–7959. doi: 10.1002/chem.201003702
- [56] Laine, T. M., Kärkäs, M. D., Liao, R.-Z., Siegbahn, P. E. M., Åkermark, B. A dinuclear ruthenium-based water oxidation catalyst: Use of non-innocent ligand frameworks for promoting multi-electron reactions. *Chem. Eur. J*, 2015. 21: pp. 10039–10048. doi: 10.1002/chem.201406613
- [57] Berardi, S., Francàs, L., Neudeck, S., Maji, S., Benet-Buchholz, J., Meyer, F., Llobet, A. Efficient light-driven water oxidation catalysis by dinuclear ruthenium complexes. *ChemSusChem*, 2015. 8: pp. 3688–3696. doi: 10.1002/cssc.201500798
- [58] Sens, C., Romero, I., Rodríguez, M., Llobet, A., Parella, T., Benet-Buchholz, J. A new Ru complex capable of catalytically oxidizing water to molecular dioxygen. *J. Am. Chem. Soc*, 2004. 126: pp. 7798–7799. doi: 10.1021/ja0486824
- [59] Bozoglian, F., Romain, S., Ertem, M. Z., Todorova, T. K., Sens, C., Mola, J., Rodríguez, M., Romero, I., Benet-Buchholz, J., Fontrodona, X., Cramer, C. J., Gagliardi, L., Llobet, A. The Ru-hbpp water oxidation catalyst. *J. Am. Chem. Soc*, 2009. 131: pp. 15176–15187. doi: 10.1021/ja9036127
- [60] Lewandowska-Andralojc, A., Polyansky, D. E., Zong, R., Thummel, R. P., Fujita, E. Enabling light-driven water oxidation via a low-energy Ru^{IV}=O intermediate. *Phys. Chem. Chem. Phys*, 2013. 15: pp. 14058–14068. doi: 10.1039/C3CP52038B
- [61] Polyansky, D. E., Muckerman, J. T., Rochford, J., Zong, R., Thummel, R. P., Fujita, E. Water oxidation by a mononuclear ruthenium catalyst: Characterization of the intermediates. *J. Am. Chem. Soc*, 2011. 133: pp. 14649–14665. doi: 10.1021/ja203249e
- [62] Duan, L., Fischer, A., Xu, Y., Sun, L. Isolated seven-coordinate Ru(IV) dimer complex with [HOHOH]⁻ bridging ligand as an intermediate for catalytic water oxidation. *J. Am. Chem. Soc*, 2009. 131: pp. 10397–10399. doi: 10.1021/ja9034686
- [63] Duan, L., Xu, Y., Zhang, P., Wang, M., Sun, L. Visible light-driven water oxidation by a molecular ruthenium catalyst in homogeneous system. *Inorg. Chem*, 2010. 49: pp. 209–215. doi: 10.1021/ic9017486
- [64] Wang, L., Duan, L., Tong, L., Sun, L. Visible light-driven water oxidation catalyzed by mononuclear ruthenium complexes. *J. Catal*, 2013. 306: pp. 129–132. doi: 10.1016/j.jcat.2013.06.023
- [65] Duan, L., Xu, Y., Gorlov, M., Tong, L., Andersson, S., Sun, L. Chemical and photochemical water oxidation catalyzed by mononuclear ruthenium complexes with a

- negatively charged tridentate ligand. *Chem. Eur. J.*, 2010. 16: pp. 4659–4668. doi: 10.1002/chem.200902603
- [66] Kärkäs, M. D., Åkermark, T., Johnston, E. V., Karim, S. R., Laine, T. M., Lee, B.-L., Åkermark, T., Privalov, T., Åkermark, B. Water oxidation by single-site ruthenium complexes: Using ligands as redox and proton transfer mediators. *Angew. Chem. Int. Ed*, 2012. 51: pp. 11589–11593. doi: 10.1002/anie.201205018
- [67] Kärkäs, M. D., Liao, R.-Z., Laine, T. M., Åkermark, T., Ghanem, S., Siegbahn, P. E. M., Åkermark, B. Molecular ruthenium water oxidation catalysts carrying non-innocent ligands: Mechanistic insight through structure–activity relationships and quantum chemical calculations. *Catal. Sci. Technol.*, In press. doi: 10.1039/C5CY01704A
- [68] Yu, Z., Li, F., Sun, L. Recent advances in dye-sensitized photoelectrochemical cells for solar hydrogen production based on molecular components. *Energy Environ. Sci.*, 2015. 8: pp. 760–775. doi: 10.1039/C4EE03565H
- [69] Xue, L.-X., Meng, T.-T., Yang, W., Wang, K.-Z. Recent advances in ruthenium complex-based light-driven water oxidation catalysts. *J. Photochem. Photobiol. B: Biol.*, 2015. 152: pp. 95–105. doi: 10.1016/j.jphotobiol.2015.07.005
- [70] Karlsson, E. A., Lee, B.-L., Liao, R.-Z., Åkermark, T., Kärkäs, M. D., Becerril, V. S., Siegbahn, P. E. M., Zou, X., Abrahamsson, M., Åkermark, B. Synthesis and electron-transfer processes in a new family of ligands for coupled Ru–Mn₂ complexes. *Chem-PlusChem*, 2014. 79: pp. 936–950. doi: 10.1002/cplu.201402006
- [71] Li, F., Jiang, Y., Zhang, B., Huang, F., Gao, Y., Sun, L. Towards a solar fuel device: Light-driven water oxidation catalyzed by a supramolecular assembly. *Angew. Chem. Int. Ed*, 2012. 51: pp. 2417–2420. doi: 10.1002/anie.201108051
- [72] Wang, L., Mirmohades, M., Brown, A., Duan, L., Li, F., Daniel, Q., Lomoth, R., Sun, L., Hammarström, L. Sensitizer-catalyst assemblies for water oxidation. *Inorg. Chem.*, 2015. 54: pp. 2742–2751. doi: 10.1021/ic502915r
- [73] Li, H., Li, F., Zhang, B., Zhou, X., Yu, F., Sun, L. Visible light-driven water oxidation promoted by host-guest interaction between photosensitizer and catalyst with a high quantum efficiency. *J. Am. Chem. Soc.*, 2015. 137: pp. 4332–4335. doi: 10.1021/jacs.5b01924
- [74] Frischmann, P. D., Mahata, K., Würthner, F. Powering the future of molecular artificial photosynthesis with light-harvesting metallosupramolecular dye assemblies. *Chem. Soc. Rev.*, 2013. 42: pp. 1847–1870. doi: DOI: 10.1039/C2CS35223K
- [75] Young, K. J., Martini, L. A., Milot, R. L., Snoeberger, R. C. III, Batista, V. S., Schmuttermaer, C. A., Crabtree, R. H., Brudvig, G. W. Light-driven water oxidation for solar fuels. *Coord. Chem. Rev.*, 2012. 256: pp. 2503–2520. doi: 10.1016/j.ccr.2012.03.031
- [76] Sun, J., Zhong, D. K., Gamelin, D. R. Composite photoanodes for photoelectrochemical solar water splitting. *Energy Environ. Sci.*, 2010. 3: pp. 1252–1261. doi: 10.1039/C0EE00030B

- [77] Ghosh, P. K., Brunschwig, B. S., Chou, M., Creutz, C., Sutin, N. Thermal and light-induced reduction of the ruthenium complex cation $\text{Ru}(\text{bpy})_3^{3+}$ in aqueous solution. *J. Am. Chem. Soc.*, 1984. 106: pp. 4772–4783. doi: 10.1021/ja00329a022
- [78] McNamara, W. R., Snoeberger, R. C. III, Li, G., Schleicher, J. M., Cady, C. W., Poyatos, M., Schmuttenmaer, C. A., Crabtree, R. H., Brudvig G. W., Batista, V. S. Acetylacetonate anchors for robust functionalization of TiO_2 nanoparticles with $\text{Mn}(\text{II})$ -terpyridine complexes. *J. Am. Chem. Soc.*, 2008. 130: pp. 14329–14338. doi: 10.1021/ja805498w
- [79] Zou, C., Wrighton, M. S. Synthesis of octamethylferrocene derivatives via reaction of (octamethylferrocenyl)methyl carbocation with nucleophiles and application to functionalization of surfaces. *J. Am. Chem. Soc.*, 1990. 112: pp. 7578–7584. doi: 10.1021/ja00177a020
- [80] McNamara, W. R., Milot, R. L., Song, H.-e., Snoeberger, R. C. III, Batista, V. S., Schmuttenmaer, C. A., Brudvig, G. W., Crabtree, R. H. Water-stable, hydroxamate anchors for functionalization of TiO_2 surfaces with ultrafast interfacial electron transfer. *Energy Environ. Sci.*, 2010. 3: pp. 917–923. doi: 10.1039/C001065K
- [81] Haller, I. Covalently attached organic monolayers on semiconductor surfaces. *J. Am. Chem. Soc.*, 1978. 100: pp. 8050–8055. doi: 10.1021/ja00494a003
- [82] Gillaizeau-Gauthier, I., Odobel, F., Alebbi, M., Argazzi, R., Costa, E., Bignozzi, C. A., Qu, P., Meyer, G. J. Phosphonate-based bipyridine dyes for stable photovoltaic devices. *Inorg. Chem.*, 2001. 40: pp. 6073–6079. doi: 10.1021/ic010192e
- [83] Brown, D. G., Schauer, P. A., Borau-Garcia, J., Fancy, B. R., Berlinguette, C. P. Stabilization of ruthenium sensitizers to TiO_2 surfaces through cooperative anchoring groups. *J. Am. Chem. Soc.*, 2013. 135: pp. 1692–1695. doi: 10.1021/ja310965h
- [84] Bae, E., Choi, W., Park, J., Shin, H. S., Kim, S. B., Lee, J. S. Effects of surface anchoring groups (carboxylate vs phosphonate) in ruthenium-complex-sensitized TiO_2 on visible light reactivity in aqueous suspensions. *J. Phys. Chem. B*, 2004. 108: pp. 14093–14101. doi: 10.1021/jp047777p
- [85] Park, H., Bae, E., Lee, J.-J., Park, J., Choi, W. Effect of the anchoring group in Ru-bipyridyl sensitizers on the photoelectrochemical behavior of dye-sensitized TiO_2 electrodes: Carboxylate versus phosphonate linkages. *J. Phys. Chem. B*, 2006. 110: pp. 8740–8749. doi: 10.1021/jp060397e
- [86] Hanson, K., Brennaman, M. K., Luo, H., Glasson, C. R. K., Concepcion, J. J., Song, W., Meyer, T. J. Photostability of phosphonate-derivatized, RuII polypyridyl complexes on metal oxide surfaces. *ACS Appl. Mater. Interfaces*, 2012. 4: pp. 1462–1469. doi: 10.1021/am201717x
- [87] Chen, Z., Concepcion, J. J., Hull, J. F., Hoertz, P. G., Meyer, T. J. Catalytic water oxidation on derivatized nanoITO. *Dalton Trans.*, 2010. 39: pp. 6950–6952. doi: 10.1039/C0DT00362J

- [88] Concepcion J. J., Jurss, J. W., Hoertz, P. G., Meyer, T. J. Catalytic and surface-electrocatalytic water oxidation by redox mediator-catalyst assemblies. *Angew. Chem. Int. Ed*, 2009. 48: pp. 9473–9476. doi: 10.1002/anie.200901279
- [89] Norris, M. R., Concepcion, J. J., Fang, Z., Templeton, J. L., Meyer, T. J. Low-overpotential water oxidation by a surface-bound ruthenium-chromophore–ruthenium-catalyst assembly. *Angew. Chem. Int. Ed*, 2013. 52: pp. 13580–13583. doi: 10.1002/anie.201305951
- [90] Ashford, D. L., Lapides, A. M., Vannucci, A. K., Hanson, K., Torelli, D. A., Harrison, D. P., Templeton, J. L., Meyer, T. J. Water oxidation by an electropolymerized catalyst on derivatized mesoporous metal oxide electrodes. *J. Am. Chem. Soc*, 2014. 136: pp. 6578–6581. doi: 10.1021/ja502464s
- [91] Ashford, D. L., Song, W., Concepcion, J. J., Glasson, C. R. K., Brennaman, M. K., Norris, M. R., Fang, Z., Templeton, J. L., Meyer, T. J. Photoinduced electron transfer in a chromophore–catalyst assembly anchored to TiO₂. *J. Am. Chem. Soc*, 2012. 134: pp. 19189–19198. doi: 10.1021/ja3084362
- [92] Song, W., Ito, A., Binstead, R. A., Hanson, K., Luo, H., Brennaman, M. K., Concepcion, J. J., Meyer, T. J. Accumulation of multiple oxidative equivalents at a single site by cross-surface electron transfer on TiO₂. *J. Am. Chem. Soc*, 2013. 135: pp. 11587–11594. doi: 10.1021/ja4032538
- [93] Moore, G. F., Blakemore, J. D., Milot, R. L., Hull, J. F., Song, H.-e., Cai, L., Schmuttermaer, C. A., Crabtree, R. H., Brudvig, G. W. A visible light water-splitting cell with a photoanode formed by codeposition of a high-potential porphyrin and an iridium water-oxidation catalyst. *Energy Environ. Sci*, 2011. 4: pp. 2389–2392. doi: 10.1039/C1EE01037A
- [94] Glasson, C. R. K., Song, W., Ashford, D. L., Vannucci, A., Chen, Z., Concepcion, J. J., Holland, P. L., Meyer, T. J. Self-assembled bilayers on indium-tin oxide (SAB-ITO) electrodes: A design for chromophore-catalyst photoanodes. *Inorg. Chem*, 2012. 51: pp. 8637–8639. doi: 10.1021/ic300636w
- [95] Gao, Y., Ding, X., Liu, J., Wang, L., Lu, Z., Li, L., Sun, L. Visible light driven water splitting in a molecular device with unprecedentedly high photocurrent density. *J. Am. Chem. Soc*, 2013. 135: pp. 4219–4222. doi: 10.1021/ja400402d
- [96] Gao, Y., Zhang, L., Ding, X., Sun, L. Artificial photosynthesis – functional devices for light driven water splitting with photoactive anodes based on molecular catalysts. *Phys. Chem. Chem. Phys*, 2014. 16: pp. 12008–12013. doi: 10.1039/C3CP55204G
- [97] Ding, X., Gao, Y., Zhang, L., Yu, Z., Liu, J., Sun, L. Visible light-driven water splitting in photoelectrochemical cells with supramolecular catalysts on photoanodes. *ACS Catal*, 2014. 4: pp. 2347–2350. doi: 10.1021/cs500518k

- [98] Li, F., Fan, K., Wang, L., Daniel, Q., Duan, L., Sun, L. Immobilizing Ru(bda) catalyst on a photoanode via electrochemical polymerization for light-driven water splitting. *ACS Catal*, 2015. 5: pp. 3786–3790. doi: 10.1021/cs502115f
- [99] Ashford, D. L., Sherman, B. D., Binstead, R. A., Templeton, J. L., Meyer, T. J. Electro-assembly of a chromophore-catalyst bilayer for water oxidation and photocatalytic water splitting. *Angew. Chem. Int. Ed*, 2015. 54: pp. 4778–4781. doi: 10.1002/anie.201410944
- [100] Ding, X., Gao, Y., Ye, L., Zhang, L., Sun, L. Assembling supramolecular dye-sensitized photoelectrochemical cells for water splitting. *ChemSusChem*, 2015. 8: pp. 3992–3995. doi: 10.1002/cssc.201500313

